AD

Award Number: DAMD17-00-1-0500

TITLE: Novel Histone Deacetylase Inhibitors

PRINCIPAL INVESTIGATOR: Jeannine S. Strobl, Ph.D.
Anna R. Martirosyan, M.D.

CONTRACTING ORGANIZATION: West Virginia University
Morgantown, West Virginia 26506-6845

REPORT DATE: July 2002

TYPE OF REPORT: Annual

PREPARED FOR: U.S. Army Medical Research and Materiel Command
Fort Detrick, Maryland 21702-5012

DISTRIBUTION STATEMENT: Approved for Public Release;
Distribution Unlimited

REPORT DOCUMENTATION PAGE

Form Approved
OMB No. 074-0188

1. AGENCY USE ONLY (Leave blank)	2. REPORT DATE	3. REPORT TYPE AND DATES COVERED
	July 2002	Annual (15 Jun 01 - 14 Jun 02)

4. TITLE AND SUBTITLE
Novel Histone Deacetylase Inhibitors

5. FUNDING NUMBERS
DAMD17-00-1-0500

6. AUTHOR(S)
Jeannine S. Strobl, Ph.D.
Anna R. Martirosyan, M.D.

7. PERFORMING ORGANIZATION NAME(S) AND ADDRESS(ES)

West Virginia University
Morgantown, West Virginia 26506-6845

E-Mail: Jstrobl@hsc.wvu.edu

8. PERFORMING ORGANIZATION REPORT NUMBER

9. SPONSORING / MONITORING AGENCY NAME(S) AND ADDRESS(ES)

U.S. Army Medical Research and Materiel Command
Fort Detrick, Maryland 21702-5012

10. SPONSORING / MONITORING AGENCY REPORT NUMBER

11. SUPPLEMENTARY NOTES

12a. DISTRIBUTION / AVAILABILITY STATEMENT	12b. DISTRIBUTION CODE
Approved for Public Release; Distribution Unlimited	

13. ABSTRACT *(Maximum 200 Words)*

The goal of this project is to develop new drugs for cell differentiation therapy of breast cancer. Our central hypothesis is antimalarials and structurally related quinoline compounds are histone deacetylase inhibitors and cause breast tumor cell differentiation and apoptosis. We have screened 21 compounds: 9 antimalarials and 12 additional quinoline ring bearing NSC compounds. Five novel breast tumor cell differentiation agents were identified, none of which was a direct inhibitor of histone deacetylase, and therefore promote breast tumor cell differentiation by novel mechanism(s). Two new histone deacetylase inhibitors were identified. Four (NSC 10010, NSC 305819, chloroquine and quinidine) of the 7 compounds also promoted apoptosis in cultured breast cancer cells. We conclude that these 4 quinoline ring compounds warrant further investigation as potential breast cancer therapeutic agents.

14. SUBJECT TERMS	15. NUMBER OF PAGES
breast cancer, antimalarials, quinolines, differentiation	63
	16. PRICE CODE

17. SECURITY CLASSIFICATION OF REPORT	18. SECURITY CLASSIFICATION OF THIS PAGE	19. SECURITY CLASSIFICATION OF ABSTRACT	20. LIMITATION OF ABSTRACT
Unclassified	Unclassified	Unclassified	Unlimited

NSN 7540-01-280-5500

Standard Form 298 (Rev. 2-89)
Prescribed by ANSI Std. Z39-18
298-102

Table of Contents

<u>Text Annual Report DAMD17-00-1-0500 Year 2</u>

Introduction

Histone deacetylases (HDAC) are a family of enzymes that modify chromatin structure, transcription factor acetylation status, and regulate gene expression. Interest in HDAC as a target for anti-cancer drug development is based upon the antiproliferative activity of HDAC inhibitors in tissue culture cell lines and their anti-tumor properties in transplanted tumors in animals. We are engaged in a drug screening process to identify antimalarial drugs, and drugs with analogous quinoline ring chemical structures, that exhibit antiproliferative activity in human breast cancer cell lines, MCF-7 and MDA-MB-231. While we have identified only one new compound that causes direct inhibition of the HDAC enzyme, we have identified many quinoline ring compounds that cause growth arrest, differentiation, and apoptosis in human breast cancer cells. The significance of this work is that it provides the basis for development of novel breast cancer therapeutic agents that act to promote cellular differentiation of breast tumor cells.

Body

Task 1 – complete
Task 2 – complete
Task 3 – complete
Task 4 –

1. <u>Histone Deacetylase (HDAC) assays</u> were completed for a total of 24 compounds (15 NSC compounds in the NCI database and 9 compounds in the antimalarial class). Three other NSC compounds were inactive in our proliferation assays and were dropped from further study. The HDAC assay results are summarized in Figure 1. Trichostatin A (TSA), a direct HDAC inhibitor was used as the positive control in these studies. We conclude that antimalarial compounds and other antiproliferative quinoline compounds are not generally direct inhibitors of HDAC.
2. <u>Ki 67 Index Assays</u> Twenty-two compounds were screened for cell differentiation activity using the Ki67 index. Ki67 index was defined as the ratio of Ki67 negative cells in Drug treated: Control cell cultures. Ki67 is a nuclear antigen that is expressed by all cells engaged in the cell cycle, but is lost once cells exit the cell cycle into G0. Therefore, the greater the Ki67 index number, the greater the differentiating power of the drug. (Because some compounds induced Oil Red O positive lipid droplets without promoting exit from the cell cycle as measured using the Ki67 index, we elected to use Ki67 immunoreactivity rather than Oil Red O staining to evaluate the differentiation potential of these compounds). The Ki67 index studies are summarized in Figure 2, and are the average Ki67 index in a minimum of 3 experiments/compound +/- SE. Tests with several of the drugs are being replicated (10010,2039,86372,4239, 3852, 124637, and hydroxychloroquine) to reconcile interassay variations. At the present time, the Ki67 index for 7 compounds was greater than 5, indicating that the drug treatment reduced the fraction of cells engaged in the cell cycle from ~95% to 19% or less. We conclude that compounds with a Ki67 index of ≥ 5 have the greatest potential as cell differentiation agents. These compounds are 10010 (4 uM), 3852 (10 uM), chloroquine (33 uM), quinidine (110uM), 69603 (14 uM), 305819 (8 uM), 86371 (5.7uM). All of these drugs were active differentiation agents at or below the IC50 for inhibition of MTS metabolism (proliferation assay). Two of these, NSC 3852 (10 uM) and NSC 86371 (5.7 uM), showed activity as a direct HDAC inhibitors. Therefore, we have identified five compounds that inhibit proliferation of breast tumor cell lines and cause cellular differentiation by a mechanism, distinct from the known direct HDAC inhibitory cell differentiation agents (e.g. TSA).
3. <u>Cellular Apoptosis assays</u> were completed in MCF-7 cells exposed for 48 and 72 h to the compounds in the antimalarial class. The nucleosome release ELISA used in these experiments detects the release of nucleosomal fragments into the cytoplasm.

Etoposide (30 μM) was used as the positive control for these assays. Of the nine compounds in the antimalarial class (amodiaquin, quinolinic acid, quinoline, primaquine, mefloquine, quinine, halofantrine, quinidine and chloroquine), only quinidine and chloroquine induced a statistically significant apoptotic response at concentrations that inhibit MTS metabolism by 50% (Figure 1). Only these two compounds stimulated p53 and p21/Cip1protein levels. We conclude that the antiproliferative and the differentiating activity of compounds in this class are independent of the apoptotic response. Induction of p53 suggested that chloroquine and quinidine might induce DNA damage and that damage was required to trigger apoptosis. Chloroquine was more potent and more effective than quinidine in inducing apoptosis and p21/Cip1. This data is in press (Zhou, McCracken, Strobl (2002) Control of mammary tumor cell growth in vitro by novel cell differentiation and apoptosis agents, Breast Cancer Research Treatment, in press). Cellular apoptosis assays were completed for chloroquine, 10010,hydroxychloroquine, 146397, 2039 and 3852 in the MDA-MB-231 cell line. Cells were exposed to the compounds for 24 h at the MTS IC50 level and also at 10 times the MTS IC50 level. All of the compounds induced some level of apoptosis in MDA-MB-231 cells with the rank order of effectiveness as chloroquine > 10010 >hydroxychloroquine > 146397 >2039 >3852. Preliminary results indicate that 305819 induces apoptosis in MDA-MB-231 cells, but that 69603 and 86371 do not. We conclude that chloroquine, 10010, and 305819 are promising agents because of their ability to induce cell differentiation and apoptosis in breast cancer cells. 3852 and 86371 are of interest because they inhibit HDAC inhibitor, cause cell differentiation, but fail to induce apoptosis in MDA-MB-231 cells. Further studies will be conducted to test for the ability of 10010, 305819, 69603, 86371, and 3852 to induce apoptosis in MCF-7 cells.

4. Histone Hyperacetylation assays were completed in MCF-7 cells exposed for 24 h to the compounds in the antimalarial class. Six of nine drugs in the antimalarial class increased levels of acetylated histone H4 using a Western blot assay. An alkyl amino side chain was present in all six drugs that increased H4 acetylation levels. The only drugs that increased H4 acetylation and promoted cell differentiation (Ki67 index) were quinolines substituted at the 4-position with the amino alkyl side chain (Table 1). We concluded that H4 hyperacetylation alone was insufficient to promote exit from the cell cycle, but that the 4-aminoalkyl-substituted quinoline ring is a potential pharmacophore for breast tumor cell differentiating agents.

Task 5- New objective, HDAC ubiquitination. Several attempts to demonstrate ubiquitin modification of HDAC1 in MCF-7 human breast cancer cells by Western blotting were unsuccessful.
Task 6 – not initiated yet
Task 7- dropped
Task 8- Two research manuscripts were submitted and are in press. Copies of each are included in the Appendix.

Key Research Accomplishments

Five compounds have been identified as novel breast tumor cell differentiation agents: chloroquine, quinidine, NSC 305819, NSC 69603, NSC 10010. None of these acts as a direct inhibitor of HDAC1 enzyme, and thus investigation of their mechanism(s) of action might provide insight into novel anti-cancer drug targets for development as breast cancer therapies. NSC 10010, NSC 305819, chloroquine and quinidine appear to induce apoptosis.

Two compounds have been identified as novel breast tumor cell differentiation agents that are direct inhibitors of HDAC1: NSC 3852 and NSC 86371. Preliminary assessments indicate that these compounds do not induce apoptosis in MDA-MB-231 cells.

Reportable Outcomes

Publications –

1. Melkoumian ZK, McCracken MA, Strobl JS (December, 2001). Suppression of c-Myc protein and induction of cellular differentiation in human breast cancer cells but not in normal human breast epithelial cells by quinidine, Amer. Soc. Cell Biol., Abst.#70.

2. Martirosyan A, Zhou Q, Bata RR, McCracken MA, Freeman AB, Morato-Lara C, Strobl JS (December, 2001). New pharmacologic agents promote cell differentiation in human breast tumor cells. Amer. Soc. Cell Biol., Abst.#762.

3. Zhou Q, McCracken MA, Strobl JS (2002) Control of mammary tumor cell growth in vitro by novel cell differentiation and apoptosis agents. Breast Cancer Research and Treatment, in press.

4. Melkoumian ZK, Martirosyan AR, Strobl JS (2002) Myc protein is differentially sensitive to quinidine in tumor versus immortalized breast epithelial cell lines. International J. Cancer, in press.

5. Strobl JS, Zhou Q, Martirosyan A (2002) Novel breast tumor differentiation agents. Era of Hope, 2002 DOD Breast Cancer Research Program (poster and platform session, Symp. 28)

Degrees Awarded (research support provided by this grant) –

1. Zaroui K. Melkoumian, Ph.D. in Pharmacology & Toxicology, West Virginia University, December, 2001.

2. Qun Zhou, Ph.D. in Pharmacology & Toxicology, West Virginia University, May, 2002.

3. Meredith A. McCracken, Ph.D. in Genetics and Developmental Biology, West Virginia University, May, 2002.

Funding (awarded on the basis of research supported by this grant) –

1. DAMD17-02-1-0622, "Augmentation of the Differentiation Response to Antitumor Antimalarials", Rayhana Rahim Bata (PI), J. Strobl (coPI), Predoctoral Fellowship, 2002-2005, $66,000.

Employment/Research Opportunities –

1. Dr. Melkoumian, Postdoctoral Fellow, Cancer Research Laboratory, Cornell University, Ithaca, NY.
2. Dr. Zhou, Cancer Research Fellow, Mary Babb Randolph Cancer Center, Morgantown, WV
3. Dr. Meredith McCracken, Postdoctoral Fellow, Dept. of Radiation Oncology, University of Michigan, Ann Arbor.
4. Mr. Andrew Freeman – summer research student (will enter WVU School of Medicine, 08/02) – salary and research support.
5. Ms. Rachael Howard – summer undergraduate student (will return to Washington and Jefferson College, Washington, PA, 08/02) – research support.
6. Anna Martirosyan, M.D. – Ph.D. student –salary and research support.
7. Rayhana Rahim Bata – Ph.D. student –research support.

Conclusions

We conclude that structural analogs of quinoline antimalarials hold promise for future development as cell differentiation agents for the management of breast cancer.

References - none

APPENDICES

Figure 1

Figure 2

Figure 3

Manuscript: Zhou et al, Breast Cancer Research and Treatment, 2002, in press

Manuscript: Melkoumian et al., Int. J. Cancer, 2002, in press

Abstract: Martirosyan et al., Am. Soc. Cell Biol.#762 (2001)

Abstract: Melkoumian et al., Am. Soc. Cell Biol. #70 (2001)

Abstract: Strobl et al., Era of Hope, DOD (2002)

FIGURE 1		**BREAST TUMOR DIFFERENTIATING QUINOLINES**						
07.15.02								
		Growth End-Points		**Differentiation End-Points**				
RANK	**NSC #**	**WVU**	**NCI**	**ORO**	**Histone**	**$HDAC_{activity}$**	**[ ]Ki67**	**Ki67**
		IC50	**GI50**	**Lipid Stain**	**H4-Acety.**	**Inhibitor**		
		MTS	**SRB**					
		(uM)	**(uM)**					
		Cell Line	Cell Line	Cell Line	Cell Line	HeLa X-tract		
		1 2	1 2	1 2	1 2			
1	86372	.14 .17	.12 .16	N N		N		
2	4238	.31 .88	1.6 .85	Y Y		N	.35uM	1.9+/-0.4
3	146397	.88 1.8	1.1 2.6	Y N		N	.9uM	2.3+/-0.6
4	4239	1.0 .39	2.3 5.9	Y Y		N	.66uM	2.4+/-0.6
5	85701	2.8 .46	4.2 nd	Y N		N	4.37uM	2.7+/-1.0
6	**157387**	3.0 nd	nd nd	Y Y		N	3.8uM	0.3+/-0.2
7	**149765**	3.4 >100	16.4 43.7	Y N	Y N	N	3.0 uM	1.1+/-0.2
8	86371	5.7 1.1	nd nd	Y Y		Y	5.7uM	6.0+/-0.9
9	10010	6.5 .72	5.4 1.27	Y Y		N	4 uM	8.3+/-4.9
10	85700	6.5 nd	7.4 33.2			N	6.5uM	4.1+/-0.5
11	**Amodiaquin**	6.9 nd	nd nd	Y Y	Y	N	7 uM	2.4+/-0.4
12	305819	7.9 3.9	12.6 9.4	Y Y		N	7.9uM	5.8+/-3.1
13	**305789**	10.7 ND	10.2 2.5	Y Y		N	10 uM	1.4+/-0.2
14	2039	12.7 7.3	1.7 3	? WEAK		N		
15	86373	12.9 ?	nd nd	Y Y		N	12.9uM	4.7+/-2.9
16	3852	14 1.8	1.8 6.4	Y WEAK		Y	10uM	8.5+/-1.3
17	69603	14.4 .85	.85 .57	Y Y		N	14.4uM	6.0+/-2.3
18	QuinolinicAcid	28.2 nd	nd nd	WEAK ?		N	30 uM	0.4+/-0.1
19	**14050**	32.8 10.8	19 16	Y Y	Y	N	35 uM	6.5+/-3.7
20	**5362**	40.1 nd	60 100	Y Y	Y	N	40 uM	4.1+/-0.5
21	**Hdrxy/clq**	56.6 27.9	nd nd	Y Y		N	56.6uM	2.4+/-2.0
22	Quinoline	61.5 nd	nd nd	N ND		N	62 uM	0.44+/-0.1
23	**Quinidine**	113.6 nd	nd nd	Y Y	Y	N	110 uM	5.0+/-1.8
24	249913	INACTIVE	nd nd					
25	15783	INACTIVE	4.3 16.1					
26	339004	INACTIVE	45.3 70					
27	124637	Not Tested	13.6 17					
	TSA	35nM nd		Y ND	Y	Y		1.6, 3.3
Legend	Compounds are ranked based on growth inhibition in the MTS (tetrazolium dye assay)							
	and the SRB(sulforhodamine dye ssay). Compounds in **bold** are antimalarial drugs.							
	149765 = Primaquine; 157387 = Mefloquine; 5362 = Quinine; 14050 = Chloroquine;							
	305789 = Halofantrine							
	Cell line 1 = MCF-7		Cell line 2 = MDA-MB-231.			nd= not determined		
	ORO = Oil Red O		Histone H4 Acetylation was measured by Western blot					
	HDAC activity was measured using BioMol Fluor d Lys assay kit.							
	KI67 = Negative cell # Drug/Ctrl			MCF-7 cells				

Fig. 2

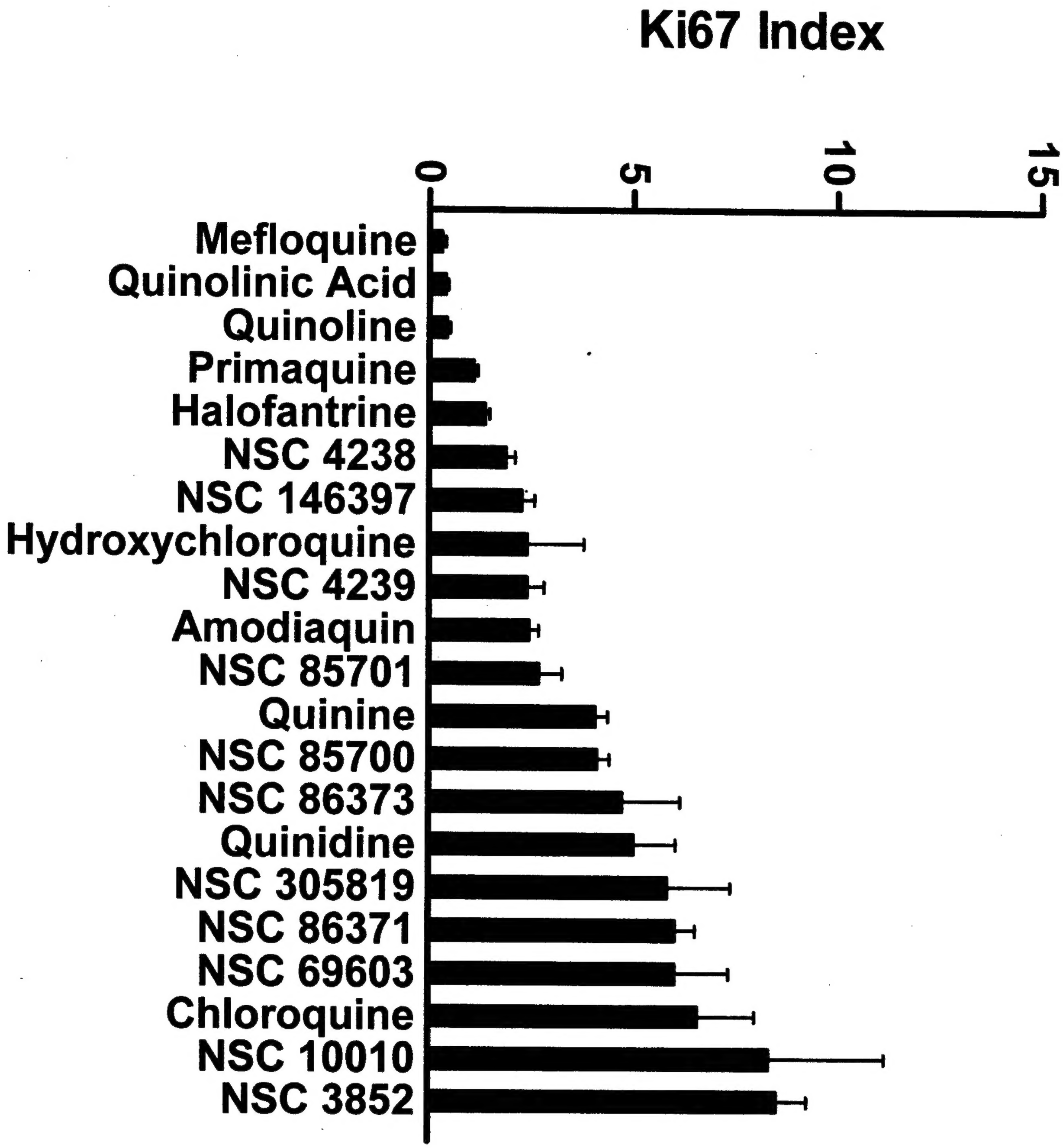
Ki67 Index
0
5
10
15
Mefloquine
Quinolinic Acid
Quinoline
Primaquine
Halofantrine
NSC 4238
NSC 146397
Hydroxychloroquine
NSC 4239
Amodiaquin
NSC 85701
Quinine
NSC 85700
NSC 86373
Quinidine
NSC 305819
NSC 86371
NSC 69603
Chloroquine
NSC 10010
NSC 3852

Fig. 3

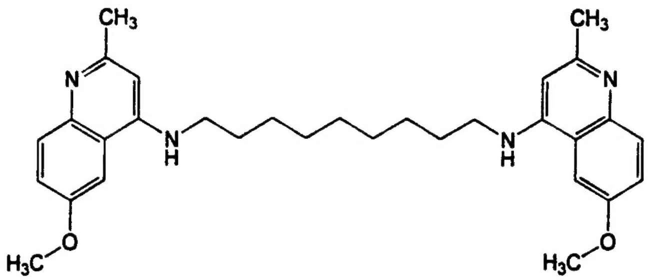

NSC 10010

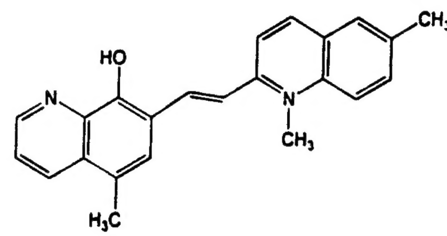

NSC 86371

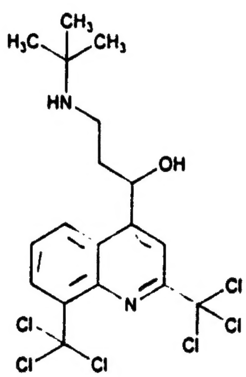

NSC 305819

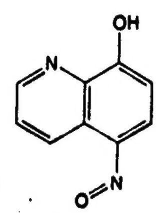

NSC 3852

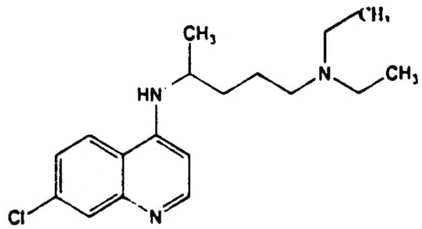

CHLOROQUINE

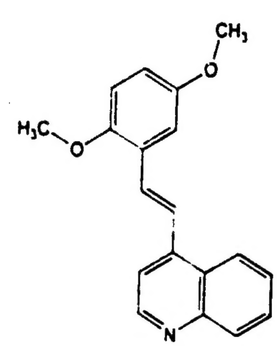

NSC 69603

Breast Cancer Research and Treatment **2345-01:** 1–11, 2002.

Report

Control of mammary tumor cell growth *in vitro* by novel cell differentiation and apoptosis agents

FIRST PROOF

Qun Zhou[1], Meredith A. McCracken[2], and Jeannine S. Strobl[1,2]
[1]*Department of Biochemistry and Molecular Pharmacology,* [2]*Genetics and Developmental Biology Program, West Virginia University, Morgantown, WV, 26506, USA*

Key words: apoptosis, breast cancer, cell differentiation agents, chloroquine, MCF-7, quinidine, quinine

Summary

The use of breast tumor differentiating agents to complement existing therapies has the potential to improve breast cancer treatment. Previously we showed quinidine caused MCF-7 cells to synchronously arrest in G1 phase of the cell cycle, transition into G0 and undergo progressive differentiation. After 72–96 h cells became visibly apoptotic. Using several analogs of quinidine we determined that MCF-7 cell cycle exit and differentiation are typical of quinoline antimalarial drugs bearing a tertiary amine side chain (chloroquine, quinine, quinidine). Differentiated cells accumulated lipid droplets and mammary fat globule membrane protein. Apoptosis was assayed by a nucleosome release ELISA. Quinidine and chloroquine triggered apoptosis, but not quinine, a quinidine stereoisomer that displayed weak DNA binding. The apoptotic response to quinidine and chloroquine was p53-dependent. A 4–15-fold induction of p21(WAF1) protein was observed in cells treated with quinidine or chloroquine prior to apoptosis, but p21(WAF1) was not increased in cells that differentiated in response to quinine. Chloroquine was most active in stimulating MCF-7 apoptosis, and quinine was most active in promoting MCF-7 cell differentiation. We conclude, distinct mechanisms are responsible for breast tumor cell differentiation and activation of apoptosis by quinoline antimalarials. Alkylamino-substituted quinoline ring compounds represented by quinidine, quinine, and chloroquine will be useful model compounds in the search for more active breast tumor differentiating agents.

Introduction

Our laboratory is investigating the use of quinoline antimalarials as inexpensive drugs with low toxicity for adjuvant breast cancer treatment. Quinidine is a natural alkaloid that is derived from the bark of the cinchona tree. Quinidine is used therapeutically to treat cardiac arrhythmia and malaria. Quinine is present in cinchona tree bark in even higher concentrations than quinidine. Quinine has antimalarial activity equivalent to that of quinidine but is not used as an antiarrhythmic agent [1]. Interestingly, quinidine and quinine are stereoisomers (Figure 1). In quinidine, the secondary alcohol of the side-chain in the 4-position of the quinoline ring is the dextrorotary conformation while in quinine the 4-hydroxyl group exists in the levorotatory conformation. The synthetic alkaloid, chloroquine is a more potent antimalarial than either quinidine or quinine. Chloroquine is a 4-alkylamino substituted quinoline that also possesses a chlorine substitution at the 7-position of the ring. Despite chloroquine's structural similarities with quinine and quinidine, chloroquine has a different mechanism of antimalarial activity, and chloroquine-resistant malaria responds to quinine treatment. The quinoline ring by itself lacks antimalarial or antiarrhythmic activity indicating that therapeutic properties are conferred by the side chain substituents. This group of pharmacologically active compounds might have anticancer properties.

We reported previously that quinidine causes moderate growth arrest and morphologic differentiation of human breast cancer cells *in vitro* [2–4]. In an experiment which compared MCF-7 cell numbers after 5

Spare set - for your information only, please retain

AUTHOR'S PROOF

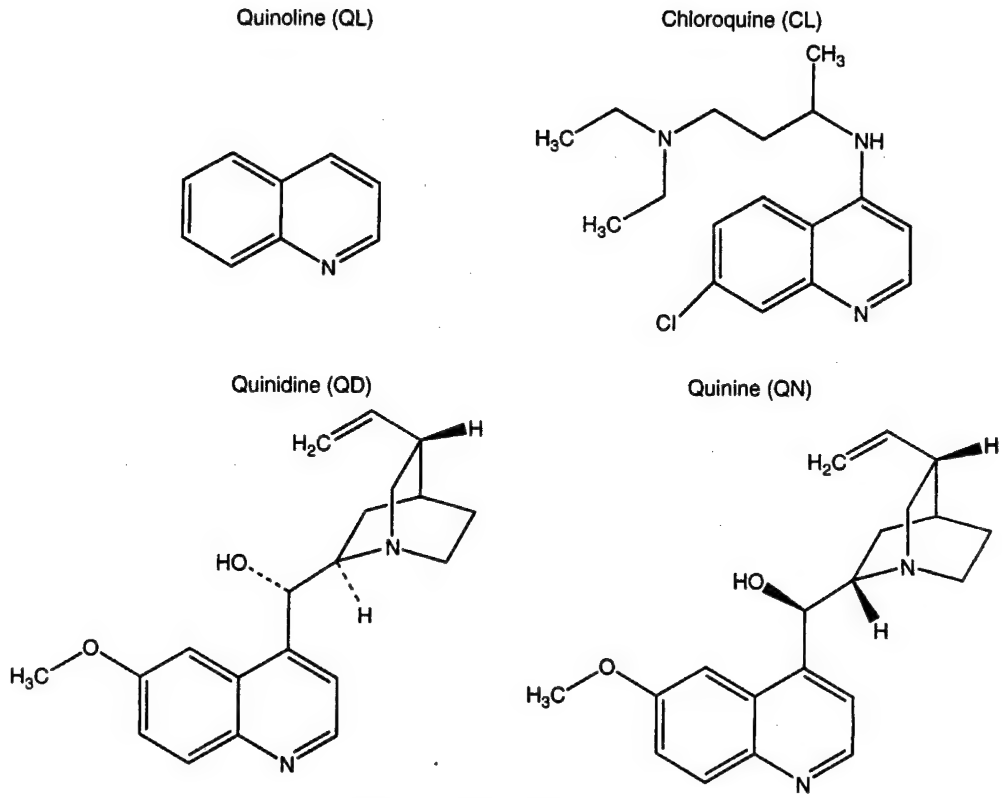

Figure 1. Structures of antimalarials.

days growth in the presence and absence of quinidine, 25 μM quinidine was found to reduce the increase in cell numbers by 50% [2]. Quinidine promoted cell cycle arrest in G1, exit into G0 marked by a loss of expression of Ki67 antigen, and lipid droplet accumulation and cytoplasmic enlargement, morphological evidence of cellular differentiation [3, 4]. Accumulation of MCF-7 cells in the G1/G0 phase of the cell cycle was maximal between 24 and 48 h with 90 μM quinidine. The potassium channel blocking activity of quinidine is implicated in the G1 arrest of MCF-7 cells, although the signaling pathway has not yet been elucidated [3]. The mechanism of quinidine action on growth in MCF-7 cells involves a number of changes in cell cycle proteins that regulate progression through G1 phase [4, 5]. Quinidine (90 μM) treatment caused increased p21(WAF1), p53, and p27 protein levels, and decreased cyclin D1, phosphorylated pRb, and Myc. Quinidine also raised levels of acetylated histone H4, a response that has been correlated with cellular differentiation in breast tumor cells [4, 6]. The differentiation response to quinidine in MCF-7 cells was well developed by 48–72 h. In cells continously exposed to quinidine for 72–96 h, apoptotic nuclei stained with Hoechst dye were apparent [3], suggesting that quinidine causes both growth arrest, via cell cycle arrest and differentiation, and cell death.

The present report describes the results of a comparative study of the effects of quinidine, quinoline and two additional quinoline antimalarials, quinine and chloroquine on MCF-7 cell apoptosis and differentiation. Our data show that quinoline antimalarials inhibit growth of human breast cancer cells *in vitro* and support the hypothesis that quinoline antimalarials cause cellular differentiation and apoptosis via distinct pathways.

Materials and methods

Chemicals

Chloroquine (CL), Oil Red O (ORO), quinidine (QD), quinine (QN), quinoline (QL) and trichostatin A (TSA) were purchased from Sigma Chemical Company (St. Louis, MO).

Tissue culture

Permanent cell lines derived from patients with breast carcinoma were used in these studies. MCF-7 cells between passage numbers 30–50, MCF-7ras, T47D and MDA-MB-231 cells were maintained in Dulbecco's Modified Eagle's medium (DMEM) (BioWhittaker, Walkersville, MD) supplemented with 10% heat-inactivated fetal bovine serum (FBS) (Hyclone Laboratories, Inc., Logan, Utah), and 40 ug/ml gentamicin. Experiments were performed in DMEM/5%FBS. The cells were cultured at 37°C in a humidified atmosphere of 93% air/7% CO_2.

MTS (3-(4,5-dimethylthiazol-2-yl)-5-(3-carboxymethoxyphenyl)-2-(4-sulfophenyl)-2H-tetrazolium) assay

MCF-7 cells were plated at 4.0×10^3 cells/well in 96-well plates in 225 μl of DMEM/5% FBS. Twelve hours after plating, the test agents were added and the cells were incubated for an additional 48 h. Cell growth was measured using a MTS assay kit (Cell-Titer 96 AQueous one solution assay, Promega, Madison, WI) according to the manufacturer's instructions. Assays were repeated at least three times. The concentration of each agent that inhibited cell growth by 50% (IC50) was determined using non-linear regression analysis to fit the inhibition data (Prism 3.0, GraphPad Software, Inc., San Diego, CA).

Ki67 immunohistochemical assay

An immunohistochemical assay for Ki67 antigen was performed according to the protocol described by Wang et al. [3]. MCF-7 cells (2×10^5/dish) were plated on ethanol-washed glass coverslips in 35 mm^2 dishes. Twelve hours after plating, test compounds were added to the medium using the IC50 determined in the MTS assay. Forty-eight hours later, the cells were fixed in acetone:ethanol (50:50) on ice for 10 min, and washed with PBS-0.15% bovine serum albumin (BSA, fraction V, Sigma) (PBS-BSA). Cells were incubated for 10 min with 0.3% hydrogen peroxide in methanol, rinsed with PBS-BSA, and incubated for 30 min with 10% horse serum in PBS-BSA. Cells were incubated for 60 min with the primary antibody Ki67 (MIB-1, Dako Corporation, Glostrup, Denmark) diluted in PBS-BSA (1:77). After rinsing with PBS-BSA, the secondary antibody, biotinylated horse anti-mouse IgG (Vector Laboratories, Burlingame, CA) diluted in PBS-BSA (1:250) was added for 30 min. The cells were rinsed with PBS-BSA and incubated for 30 min with the avidin-biotin-peroxidase reagent (Vector Laboratories). After rinsing with PBS, the antigen-antibody complexes were visualized using diaminobenzidine (Stable DAB, Research Genetics, Huntsville, AL). The cells were counterstained with Mayer's hematoxylin (Fisher Scientific, Pittsburgh, PA), and the coverslips mounted using Permount (Fisher). Ki67 negative cells were visualized by light microscopy (400 × objective, Ortholux microscope, Ernst Leitz, Wetzlar, Germany). The percentage of Ki67 negative cells in a population of at least 500 cells per experimental condition was determined.

Oil red O assay

Lipid droplet accumulation in the cytoplasm was measured using Oil Red O (ORO) staining [7]. MCF-7 cells (1×10^5 per dish) were plated on ethanol-washed glass coverslips in 35 mm^2 dishes. Cells were treated with drug or vehicle for 48–72 h, fixed in 10% formaldehyde-0.2% calcium acetate in PBS for 3 min and stained for 10 min using the ORO stock solution (0.5% ORO in 98% isopropanol) diluted 6:4 in distilled water. The coverslips were rinsed in tap water, counterstained with Mayer's Hematoxylin solution, and mounted using 50:50 (v/v) glycerol/water. Lipid droplet accumulation was visualized by light microscopy (400 ×). Positive ORO cells had at least 10 lipid droplets per cell. The percentage of positive ORO cells was determined by counting at least 300 cells per experimental condition.

Western blotting

Cells were harvested from confluent T-75 flasks and subcultured (1×10^6) in 100 mm^2 dishes. Cell lysates were prepared by scraping cells into ice-cold harvesting buffer (1% SDS-10 mM Tris–HCl, pH 7.4). The lysates were boiled for 5 min, and protease inhibitors added (Protease Inhibitor Mixture, Roche Applied Sciences, Indianapolis, IN). The supernatants were collected after centrifugation in an Eppendorf microcentrifuge (14,000 rpm, 5 min) at 4°C. The protein concentration of the supernatant was determined using a BCA protein assay (Pierce, Rockford, IL) and BSA as a standard. Equal amounts of protein were loaded onto 12% SDS-polyacrylamide mini-gels. Colored

molecular weight protein markers (Amersham Pharmacia Biotech Inc., Piscataway, NJ) were used to estimate the molecular weight of the immunoreactive proteins. Proteins were transferred to polyvinylidene difluoride membranes (PVDF, Invitrogen, Carlsbad, CA) and blocked overnight at 4°C using 3% non-fat milk blocking buffer (3 g non-fat dry milk per 100 ml of TBS (20 mM Tris–HCl, pH 7.5, 0.5 M NaCl) and 0.05% (v/v) Tween 20). Membranes were incubated for 3 h at room temperature with the following primary antibodies: mouse monoclonal anti-p21 (WAF1) (Ap-1), mouse monoclonal anti-p53 (Ap-5) (Oncogene, Cambridge, MA) or mouse anti-human milk fat globule membrane (MFGM) protein (MAB-4043, Chemicon International, Temecula, CA). The primary antibodies were diluted 1 : 500 in Western washing solution (0.1% non-fat dry milk, 0.1% albumin (chicken egg), 1% (v/v) FBS, 10% (v/v) of 10 × PBS, pH 7.3, 0.2% (v/v) Tween-20). After washing three times with Western washing solution and one time with TBS, the antigen-antibody complexes were incubated 1 h at room temperature with HRP (horseradish peroxidase)-conjugated secondary antibody (anti-mouse IgG-HRP, Santa Cruz Biotechnology) diluted 1 : 3000 in Western washing solution. After washing three times with TBS, antibody binding was visualized using enhanced chemiluminescence (SuperSignal West Pico, Pierce) and autoradiography.

Densitometric analysis

Autoradiograms of the Western immunoblots were scanned using ChemiImager software (Alpha Innotech Corporation, San Leandro, CA). The blots were adjusted for brightness and contrast, and the mean density for each band was analyzed using ChemiImager analysis program. The background value was subtracted from each individual object.

Cell death ELISA (enzyme-linked immunosorbent assay)

Apoptotic cells were measured using the cell death ELISA kit (Roche Applied Science). Cells (4.0×10^3) were plated in each well of 96-well plates and treated in triplicate with either drug or vehicle (control cells) for 48 or 72 h. Cell cytoplasmic fractions were prepared and 20 µl aliquots were transferred into streptavidin-coated microtiter plates (MTP) for analysis as per the instructions of the supplier. Apoptosis, measured as nucleosome release into the cytoplasmic fraction, was quantified spectrophotometrically (A_{405} nm, EL340 Biokinetics Reader, Bio-Tek Instruments, Winooski, Vermont) using ABTS (2,2-Azino-di-3-ethylbenzthiazolin-sulfonat) as the substrate.

P21(WAF1) ELISA

Cells were plated (1×10^6 cells/100 mm^2 dish); 12 h later MTS IC50 of each test agent were added to the medium and incubated for 24 h. Fifty micrograms protein aliquots of the cell lysates were assayed for p21(WAF1) using a colorimetric ELISA (Oncogene, Boston, MA) according to the manufacturer's instructions.

DNA binding assay

Chloroquine, quinidine, and quinine emit an intense blue fluorescence when excited by ultraviolet light [8]. Intercalation into DNA quenches the chloroquine fluorescence [9], and this principle is the basis of the fluorescence assay we used to assess DNA binding by quinidine and quinine. Stock solutions of chloroquine, quinidine, and quinine in water were diluted 1 : 1 in 10 mM Tris, 1 mM EDTA, pH 8 (TE) or TE containing 1 µg of lambda DNA (Invitrogen, Carlsbad, CA) to a final concentration of 100 µg drug/ml. The final reaction volume was 20 µl. Drugs or drugs plus DNA were incubated for 15 min at room temperature in the dark in a 96-well plate (Nunc Immunoplate, Nunc Nalge International). Fluorescence was then measured using a CytoFluor4000 (PerSeptive Biosystems) instrument using an excitation wavelength of 360 nm and an emission wavelength of 460 nm. Background fluorescence from TE alone or TE plus DNA samples was subtracted from each measurement as appropriate. Data were expressed as the fluorescence quench ratio defined as the average fluorescence of drug alone (Em1) divided by that of drug in the presence of DNA (Em2).

Statistical analysis

Data are expressed as the mean ± SE for n number of replicates as indicated in the figure legends. One-way ANOVA (analysis of variance) followed by Bonferroni's t-tests were used to assess statistically significant differences between control- and drug-treated groups (GraphPad Instat, Intuitive Software for Science, San Diego, CA).

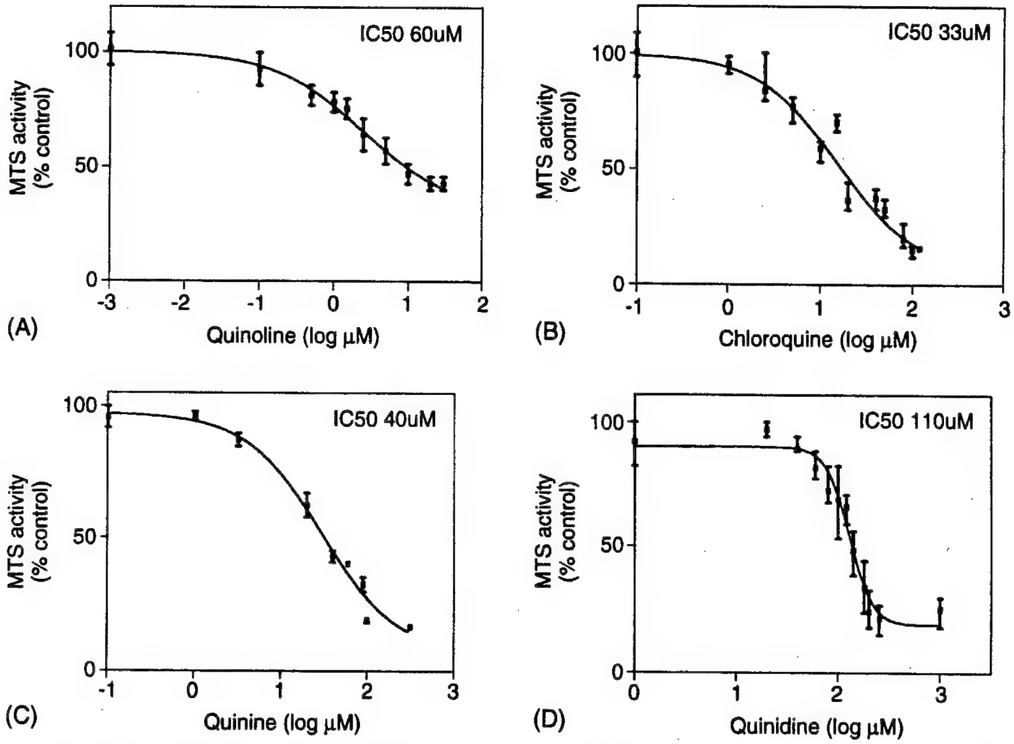

Figure 2. Antimalarials inhibited MTS metabolism in MCF-7 cells. MCF-7 cells (4000 cells/well) were grown in 96 well plates in the presence of increasing concentrations of each antimalarial for 48 h. Cell growth was estimated using the MTS assay. The IC50 value for each agent was determined using nonlinear regression analysis to fit inhibition data. Data are the mean ± SE of three independent experiments performed in quadruplicate. MTS activity of untreated cells was set 100%. The IC50 value for each antimalarial is shown in each panel.

Results

Antimalarials inhibit growth and promote MCF-7 cell differentiation

Quinidine inhibits MCF-7 cell proliferation, and to test whether this is a general response to structurally related chemicals, the effects of quinidine, quinine, chloroquine, and quinoline on MCF-7 ~~cells on~~ cell growth were compared. The MTS assay directly measures mitochondrial metabolic activity; none of the test agents directly inhibited mitochondrial metabolism of MTS after a 2 h or a 6 h exposure (data not shown). Therefore, MTS activity measured after 48 h incubation with these compounds is a valid measure of the number of surviving cells (Figure 2). The IC50 was estimated for each drug in the MTS assay, and the order of potency of the compounds was chloroquine (IC50, 33 μM) > quinine (IC50, 40 μM) > quinoline (IC50, 62 μM) > quinidine (IC50, 110 μM). The effects of chloroquine, quinine, quinoline, and quinidine on cell numbers were investigated using the IC50 values determined in the MTS assay. Chloroquine (IC50, 33 μM) caused a ~60% decrease in cell numbers after a 60 h incubation as compared with control, growing MCF-7 cells suggesting that chloroquine caused cell death. In parallel cell cultures incubated with MTS IC50 of quinoline, quinidine, and quinine, the cell numbers after 60 h did not differ from the plating density. These compounds may primarily arrest cell growth, or alternatively permit a limited amount of proliferation balanced by cell loss (Figure 3).

Earlier studies showed quinidine caused G1 arrest and exit from the cell cycle [3]. Ki67 is a nuclear protein that is expressed throughout the cell cycle. The absence of Ki67 protein is a marker for non-proliferating cells that have entered G0 phase, and, therefore, provides a means of monitoring whether cell cycle exit might contribute to growth arrest [10]. By measuring Ki67 expression immunohistochemically, chloroquine (33 μM), quinidine (110 μM), and quinine (40 μM) were shown to promote exit from the cell cycle by 48 h. Under normal culture conditions, 95% of MCF-7 cells are engaged in the cell cycle, and express Ki67 antigen; 5% of the cells in the control population were negative for immunore-

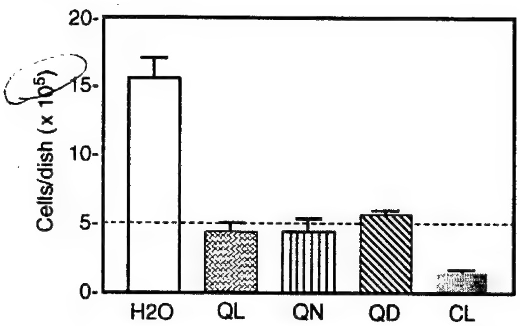

Figure 3. Effects of antimalarials on cell growth. MCF-7 cells (5×10^5) growing in 60 mm^2 dishes in DMEM/5%FBS were treated with concentrations of antimalarials corresponding to 50% inhibition of MTS activity as measured at 48 h. After 60 h incubation with antimalarials or solvent alone, viable cells that excluded trypan blue were counted using hemacytometer. Data are the mean of $n = 3 \pm$ SE independent experiments.

active Ki67 (Figure 4(A)). The percentage of Ki67 negative MCF-7 cells after 48 h growth in the presence of chloroquine, quinidine or quinine increased 6–7-fold to 30–40% compared to control cells ($p < 0.01$) (Figure 4(A)). Thus, growth inhibition by chloroquine, quinine, and quinidine can be explained in part by exit of cells from the cell cycle. Quinoline (62 μM), however, caused cell numbers to stabilize without shifting cells into G0.

Quinine, chloroquine, and quinidine also were similar in their ability to promote a more differentiated phenotype in MCF-7 cells, the accumulation of ORO positive lipid droplets in the cytoplasm [11] (Figure 4(B)). Quinoline was inactive in this assay as well. The data suggest that the stereoisomers, quinidine, and quinine act similarly, but with different potency, causing growth arrest, exit from the cell cycle and differentiation. Chloroquine was more potent and more toxic than quinidine and quinine. Chloroquine caused cell cycle exit; examination of the cells after ORO staining revealed morphologic evidence of differentiation (lipid droplets) as well as apoptotic cell death (condensed cells with heavy nuclear staining with hematoxylin Quinoline caused arrest of cell growth without promoting cell cycle exit or any evidence of differentiation. Quinoline-treated cells showed no evidence of cytotoxicity, and the mechanism for the growth arrest is unclear.

In breast cells, the human milk fat protein is another cell differentiation marker [12]. The monoclonal antibody MFGM identifies antigens found on the milk fat globule membrane, which surrounds milk fat [13]. The expression of MFGM protein was measured by western blot analysis in MCF-7 cells exposed to antimalarials for 48 h. The densitometric signals in arbitrary units derived from scanning the immunoblots

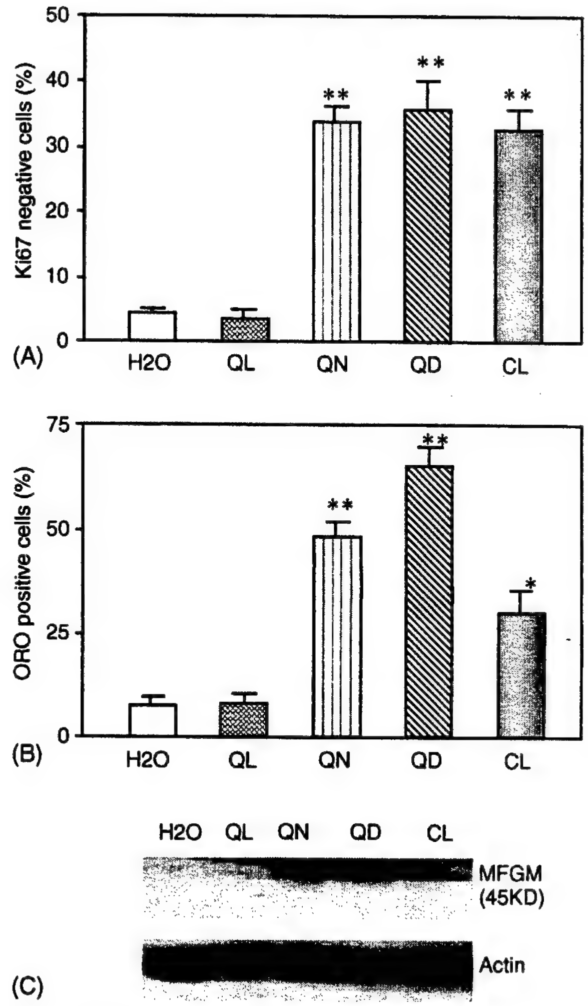

Figure 4. Cell differentiation by antimalarials. Ki67 expression, lipid droplet accumulation and human MFGM levels were measured in MCF-7 cells. MCF-7 cells were grown in 35 mm^2 dishes on sterile glass coverslips in DMEM/5%FBS. Cells were treated with solvent (distilled H_20) or the MTS IC50 of each antimalarial for 48 h (A) Ki67 immunoreactivity was performed as previously described by Wang et al. [3]. The data represent the mean percentage of Ki67 negative cells in each treatment group ($n = 3 \pm$ SE); 500 cells per experiment were counted. (B) Lipid droplet accumulation was measured using ORO staining in MCF-7 cells treated with antimalarials. The data represent the percentage ORO positive cells in each treatment group ($n = 3 \pm$ SE); 300 cells per treatment were counted. (C) Protein aliquots (25 ug) from the cell lysates were separated by 12% SDS-polyacrylamide gel electrophoresis and analyzed by western blotting using an antibody specific for MFGM. Actin protein was used as a loading control. Data are representive of two independent experiments. Statistically significant differences between control and treatment groups are indicated (*, $p < 0.05$; **, $p < 0.01$).

is provided in parantheses following each treatment. Quinidine (8872), quinine (7548), and chloroquine (8205) increased MFGM protein compared with control (5241) MCF-7 cells (Figure 4(C)). In contrast, MFGM protein levels were not changed by quinoline (5312) treatment. Changes of MFGM in MCF-7 cells by quinidine, quinine, and chloroquine are consistent with induction of lipid droplets. The coinduction of milk fat, and lipid droplets support our conclusion that quinidine, quinine, and chloroquine caused differentiation in MCF-7 cells.

Effect of antimalarials on apoptosis in MCF-7 cells

Morphological evidence that quinidine activated apoptosis in MCF-7 cells [3] prompted examination of apoptosis in cells exposed to antimalarials using the nucleosome release assay. Levels of apoptosis after 48 and 72 h were measured over a range of concentrations that spanned the respective MTS IC50 values for each compound. Etoposide (30 uM), a topoisomerase II inhibitor, elicits nucleosomal laddering in MCF-7 cells and was used as a positive control for this assay [14]. The enrichment of apoptotic response, defined as the ratio of the apotosis signal in the presence and absence of MTS IC50 concentrations of antimalarials, calculated after 48 and 72 h is summarized in Table 1. The concentration-response curve measured for each compound at 72 h is shown in Figure 5.

Quinidine and chloroquine stimulated nucleosome release in MCF-7 cells in a concentration-dependent fashion ($p < 0.05$). Chloroquine was more potent than quinidine and apoptosis was more extensive in cells exposed to chloroquine than quinidine. In contrast,

Table 1. The apoptosis enrichment factor was calculated using data obtained from ELISA, and is the ratio: units of absorbance drug treatment group/units of absorbance control group

Compounds	Apoptosis enrichment factor (mean $\pm$ SER, $N = 3$)	
	48 h	72 h
Quinoline (62 uM)	1.00 ± 0.06	1.09 ± 0.03
Quinine (40 uM)	1.13 ± 0.09	1.19 ± 0.07
Quinidine (110 uM)	1.50 ± 0.10*	1.73 ± 0.09*
Chloroquine (33 uM)	1.75 ± 0.14*	1.82 ± 0.07*
Etoposide (ET) 30 uM)	2.74 ± 0.13*	1.23 ± 0.20
Trichostatin A (35 nM)	0.96 ± 0.06	0.91 ± 0.05

Results of treatment times of 48 h and 72 h are compared.
Data shown are the mean $\pm$ SE of three experiments performed in triplicate.
*, $p < 0.05$ for drug treatment versus control.

quinoline, and quinine treatments did not change nucleosome release as compared with controls ($p > 0.05$). Quinoline displayed incomplete inhibition of MTS activity, no differentiating activity, and was not expected to activate apoptosis. However quinine inhibited MTS metabolism nearly as potently as chloroquine, and stimulated cellular differentiation. The experiments provide evidence that apoptosis, measured by nucleosome release, is differentially stimulated by the stereoisomers, quinidine, and quinine, while exit from the cell cycle, differentiation, and antimalarial activity are all stereo non-selective responses.

To investigate the stereoselectivity of the apoptotic response further, levels of p53 and a downstream target of p53, p21(WAF1), were measured in MCF-7 cells exposed for 24 h to quinidine, quinine, chloroquine or quinoline. At their MTS IC50 levels, quinidine and chloroquine elevated p53 protein in MCF-7 cells, but in cells exposed to quinine and quinoline, p53 was undetectable (Figure 6(A)). Protein p21(WAF1) was increased in chloroquine and quinidine treated cells, but not in quinine or quinoline treated cells (Figure 6(B)). An ELISA was performed on MCF-7 whole cell extracts to quantify the changes in p21(WAF1) protein in response to the antimalarials (Figure 7(A)). Trichostatin acid (TSA) was used as a positive control for these experiments. Transcription of p21(WAF1) and p21(WAF1) protein levels have been shown to be increased by TSA [15, 16]. Chloroquine caused a 10–15-fold elevation in p21(WAF1) levels in MCF-7 cells at 24 h (Figure 7(B)). The p21(WAF1) response to chloroquine exceeded that of the potent histone deacetylase inhibitor, TSA. Quinidine elevated p21(WAF1) levels 4–5-fold, approximately the same as TSA, but neither quinine nor quinoline raised p21(WAF1) protein.

Moreover, p21(WAF1) protein expression in response to quinidine (90 uM) was different in wild type p53 and mutant p53 human breast cancer cells. Quinidine treatment increased p21(WAF1) protein in MCF-7 and MCF-7ras cells (wild type p53) (Figure 8), but p21(WAF1) protein was not detectable in malignant MDA-MB-231 and T47D cells (mutant p53) using western blot analysis. We previously reported that quinidine (90 uM) induced cellular differentiation in all of these lines of breast cancer cells [4].

DNA binding by antimalarials

Chloroquine intercalates into DNA [9, 17, 18], but DNA intercalation is not required for antimalarial

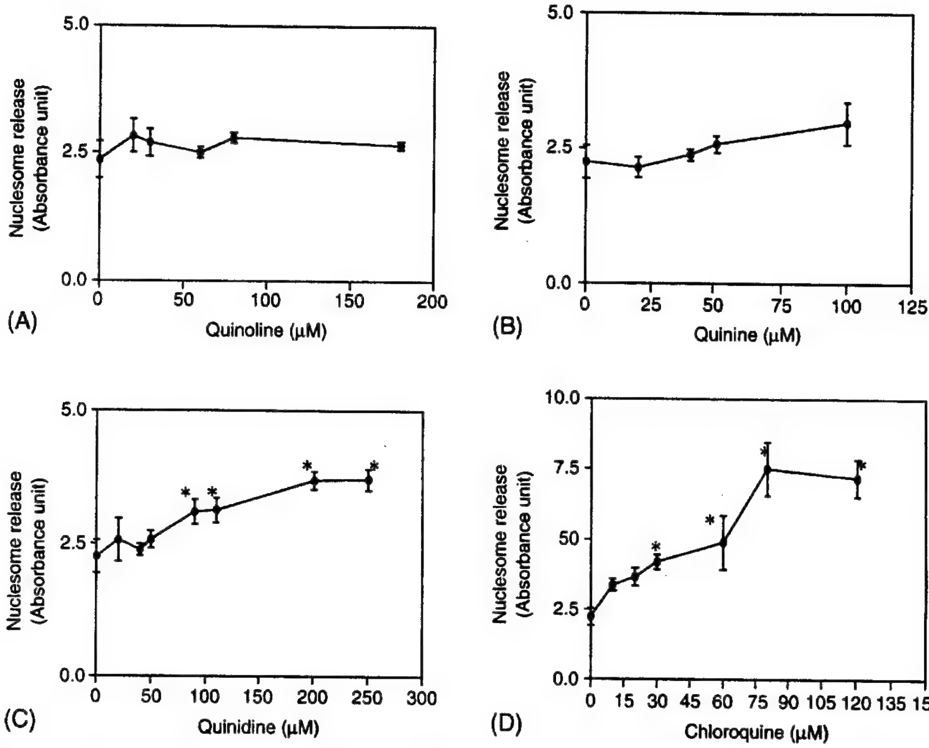

Figure 5. Nucleosome release apoptosis assay. MCF-7 cells (4000 cells/well) were grown in 96 well plates in the presence of increasing concentrations of antimalarials for 72 h. Nucleosome release was measured using the histone-DNA cell death detection kit as described in 'Materials and methods.' The level of nucleosomes released in each sample is indicated by the absorbance at 405 nm. Data are the mean ± SE of three independent experiments performed in triplicate. Statistically significant differences between control and drug treatment groups at specific drug concentrations are indicated (*, $p < 0.05$; **, $p < 0.01$). Note the change in scale of the x-axis in Panel D.

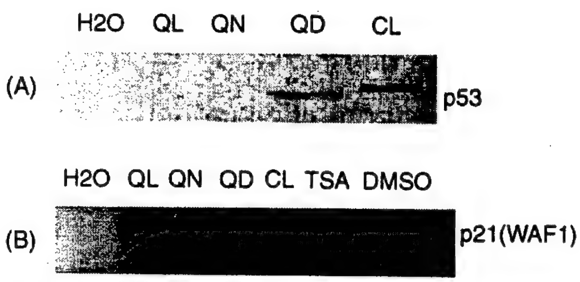

Figure 6. Western blot analysis of p21(WAF1) and p53 protein expression in human breast cancer cells. MCF-7 cells (1×10^6) were grown in 100 mm^2 dishes and treated with MTS IC50 of antimalarials for 24 h. Protein aliquots (50 μg) from the cell lysates were separated by 12% SDS-polyacrylamide gel electrophoresis and analyzed by western blotting using (A) mouse monoclonal antibody for p53. Data shown represent three independent experiments that showed the same results. (B) mouse monoclonal antibody for p21(WAF1) (single experiment). as or

activity. We hypothesize that DNA intercalation is responsible for chloroquine-induced apoptosis, and that p53 induction by chloroquine is a consequence of DNA damage arising from intercalation. Our hypothesis predicts that chloroquine and quinidine but not quinoline and quinine intercalate into DNA. The binding of chloroquine, quinidine, and quinine to DNA was measured in an *in vitro* cell-free assay. The fluorescence signal from 2 μg of free chloroquine, quinidine, and quinine dissolved in 10 mM Tris-1 mM EDTA, pH 8 was equivalent. The addition of lambda DNA to solutions of chloroquine and quinidine, but not quinine, caused a statistically significant fluorescence quenching (Figure 9). The average fluorescence quench ratio for chloroquine in four independent experiments was 2.9 while that for quinidine was 1.8. Quinine exhibited a fluorescence quench ratio of 1.1 which was not statistically significant. The results imply stereo-selective DNA binding by quinidine, and are consistent with the pattern of quinidine activation of nucleosome release, p53 and elevations in p21(WAF1) protein levels. This is the first report of quinidine binding to DNA. Using an assay that measured changes in plasmid superhelical density, quinine was reported to intercalate into DNA, however this binding is relatively weak compared to chloroquine [18].

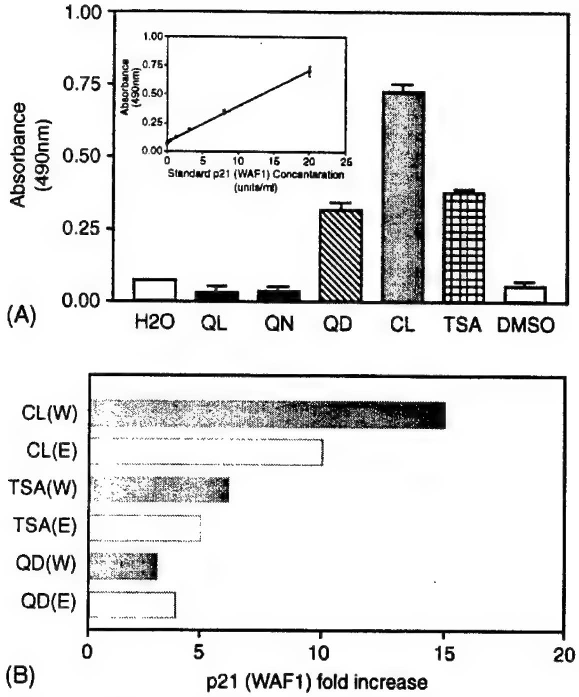

Figure 7. Effect of antimalarials on p21(WAF1) protein expression in MCF-7 human breast cancer cells. (A) p21(WAF1) ELISA. MCF-7 cells (1×10^6) were plated in $100\,mm^2$ dishes in DMEM/5% FBS, treated with solvent (distilled-H_2O or 0.01% DMSO) or MTS IC50 of each antimalarial for 24 h, and cell lysates prepared. TSA was dissolved in DMSO; antimalarials were dissolved in distilled H_2O. Proteins (50 μg) from the cell lysates were assayed using p21(WAF1) ELISA kit as detailed in 'Materials and methods' using a 20 min incubation time. Data are the mean $\pm$ SE of two independent experiments. (B) Comparison of p21(WAF1) protein changes detected in ELISA (E) and western blot analysis (W). W represents the fold increase in the signal density determined by densitometry; E represents the fold increase in absorbance in the ELISA. Fold increase is equal to drug treatment group divided by the control.

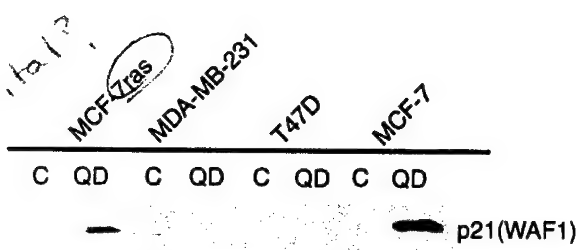

Figure 8. Effect of antimalarials on p21(WAF1) protein expression in human breast cancer cells. MCF-7, MDA-MB-231, T47D and MCF-7ras cells (1×10^6) were exposed to quinidine (90 μM) for 24 h. Protein aliquots (50 μg) from the cell lysates were separated by 12% SDS-polyacrylamide gel electrophoresis and analyzed by western blotting using mouse monoclonal antibody for p21(WAF1) (single experiment).

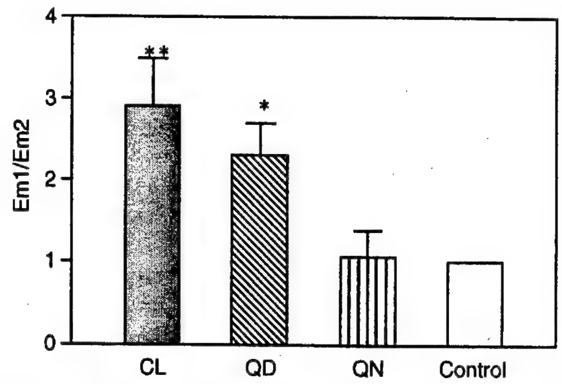

Figure 9. Fluorescence quench assay for DNA binding activity. Changes in antimalarial fluorescence upon DNA binding were measured using an excitation wavelength of 360 nm and an emission wavelength of 460 nm. Data were expressed as the fluorescence quench ratio defined as the average fluorescence of drug alone (Em1) divided by that of drug in the presence of DNA (Em2). Data represented the mean $\pm$ SE of three independent experiments. Statistically significant differences between control and treatment groups are indicated (*, $p < 0.01$; **, $p < 0.001$).

Discussion

In an effort to develop new anti-cancer therapeutic agents, we explored the anti-tumor potential of quinoline antimalarials using MCF-7 human breast cancer cells as our model system. The results of our experiments show antimalarial compounds inhibited cell growth *in vitro*, and two mechanisms for growth inhibition were identified: (1) promotion of cell cycle exit and cell differentiation and (2) activation of p53-dependent apoptosis.

Chloroquine was the most active apoptosis-inducing agent. DNA damage is a well-established apoptotic trigger that engages p53 protein as well as downstream targets of p53 including p21(WAF1) [19, 20]. Because chloroquine intercalates into DNA [21], and stimulates both p53 and p21 (WAF1) protein expression in MCF-7 cells we hypothesize that DNA damage is involved in the apoptotic response to chloroquine. The specific mechanism by which chloroquine might create DNA damage is unclear. Chloroquine is an unusual DNA intercalator because it has a two membered planar ring structure (Figure 1); in contrast, typical DNA intercalators have three or more fused planar rings [9, 21]. In addition, the tertiary aminoalkyl side-chain of chloroquine is modeled to occupy the minor groove of DNA, and this could have consequences for many DNA binding proteins and enzymes [21, 22]. Chloroquine has been reported to inhibit mammalian topoisomerase I and II [23, 24]. Inhibition of topoisomerase II activity is a clas-

sic response to DNA intercalating agents [25, 26] and topoisomerase inhibition is a potential mechanism of action of chloroquine in MCF-7 cells. Alternatively, the 10–15-fold increase in p21(WAF1) protein elicited in MCF-7 cells by chloroquine might be sufficient to activate apoptosis in the absence of DNA damage. Sheikh et al., showed that plasmid driven p21(WAF1) over expression in human breast tumor cell lines stimulated apoptosis [27]. In either this model or the DNA damage model, induction of p21(WAF1) protein emerges as a marker that can be used to screen compounds for apoptotic activity in human breast tumor cell lines.

Quinidine also increased p53 and p21 (WAF1) protein levels and stimulated apoptosis in MCF-7 cells, but was less active than chloroquine. An interesting feature of the apoptotic response of MCF-7 cells to quinidine, was the stereoselectivity. Quinine, a stereoisomer of quinidine, did not increase p53 or p21(WAF1) protein levels and did not trigger apoptotic cell death. Quinine was also less effective than either quinidine or chloroquine in binding DNA. The stereoisomers, quinine, and quinidine should prove very valuable in elucidating the mechanisms for apoptosis by quinoline drugs.

The MCF-7 response to quinine demonstrated that apoptotic cell death was not obligatory for cell growth arrest by antimalarial agents. Chloroquine, quinidine, and quinine all increased the percentage of G0 MCF-7 cells. Cell transition into the quiescent G0 phase is prerequisite for differentiation. Using lipid droplet accumulation measured by ORO staining and induction of the MFGM as markers of mammary cell differentiation, all three quinoline antimalarials were observed to induce differentiation in MCF-7 cells. Cell differentiation therapies such as FR901228, SAHA, and pyroxamide have recently entered into clinical trials and are an active area of cancer research [28, 29]. We propose on the basis of the data presented that quinoline antimalarial drugs be considered prototype compounds for the development of novel agents to stimulate breast tumor cell differentiation. Induction of differentiation by quinine was dissociated from both p21(WAF1) and apoptosis, and we conclude that differentiation is a distinct mechanism for inhibition of cell growth by antimalarials. Based on the differential response of MCF-7 cells to quinine and quinidine, we believe that a screening system based upon Ki67 expression is preferable to p21(WAF1) for identification of compounds that promote breast tumor cell differentiation.

Previous studies in our laboratory demonstrated that differentiation of MCF-7 cells by quinidine was associated with histone H4 hyperacetylation [4]. Elucidation of the regulation of histone acetylation state by antimalarials is expected to provide important insight into how quinoline antimalarials regulate breast tumor cell differentiation.

Acknowledgements

This work was supported by the Charleston Area Medical Center Foundation (8-2001), West Virginia University School of Medicine, and the US Army (DAMD 17-99-1-9449, DAMD 17-00-1-0500).

References

1. Webster Jr LT: Drugs used in the chemotherapy of protozoal infections: malaria. In: Goodman AG, Goodman LS, Rall TW, Murad F (eds) The Pharmacological Basis of Therapeutics. 7th edn MacMillan Publishing Company, NY, 1985, pp 1029–1048
2. Woodfork KA, Wonderlin WF, Peterson VA, Strobl JS: Inhibition of ATP-sensitive potassium channels causes reversible cell-cycle arrest of human breast cancer cells in tissue culture. J Cell Physiol 162: 163–171, 1995
3. Wang S, Melkoumian ZK, Woodfork KA, Cather C, Davidson AG, Wonderlin WF, Strobl JS: Evidence for an early G1 ionic event necessary for cell cycle progression and survival in the MCF-7 human breast carcinoma cell line. J Cell Physiol 176: 456–464, 1998
4. Zhou Q, Melkoumian ZK, Lucktong A, Moniwa M, Davie JR, Strobl JS: Rapid induction of histone hyperacetylation and cellular differentiation in human breast tumor cell lines following degradation of histone deacetylase-1. J Biol Chem 275: 35256–35263, 2000
5. Melkoumian ZK, Strobl JS: Myc protein is differentially sensitive to quinidine in tumor versus immortalized breast epithelial cells. Int J Cancer (in revision)
6. Munster PN, Troso-Sandoval T, Rosen N, Rifkind R, Marks PA, Richon VM: The histone deacetylase inhibitor suberoylanilide hydroxamic acid induces differentiation of human breast cancer cells. Cancer Res 61: 8492–8497
7. Graham KA, Buick RN: Sodium butyrate induces differentiation in breast cancer cell lines expressing the estrogen receptor. J Cell Physiol 136(1): 63–71, 1988
8. Udenfriend S: Drugs and toxic agents. In: Fluorescence Assay in Biology and Medicine. Vol 1, Academic Press, NY, 1962, pp 400–443
9. Hahn FE: Chloroquine. In: Corcoran JW, Hahn FE, (eds) Antibiotics, Vol III, Mechanism of Action of Antimicrobial and Antitumor Agents. Springer-Verlag Press, NY, 1975, pp 58–78
10. Van Dierendonck JH, Keijzer R, Van De Velde CJ, Cornelisse CJ: Nuclear distribution of the Ki-67 antigen during the cell cycle: comparison with growth fraction in human breast cancer cells. Cancer Res 49(11): 2999–3006, 1989

11. Bancroft JD, Cook HC: Manual of Histological Techniques. Churchill Livingstone, Edinburgh 1984, pp 132–133
12. Munster PN, Srethapakdi M, Moasser MM, Rosen N: Inhibition of heat shock protein 90 function by ansamycins causes the morphological and functional differentiation of breast cancer cells. Cancer Res 61(7): 2945–2952, 2001
13. Turnbull JE, Baildam AD, Barnes DM, Howell A: Molecular expression of epitopes recognized by monoclonal antibodies HMFG and HMFG-2 in human breast cancers: diversity, variability and relationship to prognostic factors. Int J Cancer 38(1): 89–96, 1986
14. Giocanti N, Hennequin C, Balosso J, Mahler M, Favaudon V: DNA repair and cell cycle interactions in radiation sensitization by the topoisomerase II poison etoposide. Cancer Res 53(9): 2105–2111, 1993
15. Yoshida M, Horinouchi S: Trichostatin and leptomycin. Inhibtion of histone deacetylation and signal-dependent nuclear export. Ann NY Acad Sci 886: 23–36, 1999
16. Kim YB, Ki SW, Yoshida M, Horinouchi S: Mechanism of cell cycle arrest caused by histone deacetylase inhibitors in human carcinoma cells. J Antibiot (Tokyo) 53(10): 1191–1200, 2000
17. Davidson MW, Griggs BG, Boykin DW, Wilson WD: Molecular structural effects involved in the interaction of quinoline methanolamines with DNA. Implications for antimalarial action. J Med Chem 20: 1117–1122, 1977
18. Esposito F, Sinden RR: Supercoiling in prokaryotic and eukaryotic DNA: changes in response to topological perturbation of plasmids in *E. coli* and SV40 *in vitro*, in nuclei and in CV-1 cells. Nucl Acids Res 15: 5105–5124, 1987
19. Vogelstein B, Kinzler KW: Has the breast cancer gene been found? Cell 79(1): 1–3, 1994
20. El-Deiry WS, Tokino T, Waldman T, Oliner JD, Velculescu VE, Burrell M, Hill DE, Healy E, Rees JL, Hamilton SR: Topological control of p21WAF1/CIP1 expression in normal and neoplastic tissues. Cancer Res 55(13): 2910–2919, 1995
21. O' Brien RL, Allision JL, Hahn FE: Evidence for intercalation of chloroquine into DNA. Biochim Biophys Acta 129(3): 622–624, 1966
22. Michael RO, Williams GM: Chloroquine inhibition of repair of DNA damage induced in mammalian cells by methyl methanesulfonate. Mutat Res 25(3): 391–396, 1974
23. Sorensen M, Sehested M, Jensen PB: pH-dependent regulation of camptothecin-induced cytotoxicity and cleavable complex formation by the antimalarial agent chloroquine. Biochem Pharmacol 54(3): 373–380, 1997
24. Snyder RD: Use of catalytic topoisomerase II inhibitors to probe mechanisms of chemical-induced clastogenicity in Chinese hamster V79 cells. Environ Mol Mutagen 35(1): 13–21, 2000
25. Chen AY, Liu LF: DNA topoisomerases: essential enzymes and lethal targets. Annu Rev Pharmacol Toxicol 34: 191–218, 1994
26. Solary E, Bertrand R, Pommier Y: Apoptosis induced by DNA topoisomerase I and II inhibitors in human leukemic HL-60 cells. Leuk Lymphoma 15(1–2): 21–32, 1994
27. Sheikh MS, Rochefort H, Garcia M: Overexpression of p21WAF1/CIP1 induces growth arrest, giant cell formation and apoptosis in human breast carcinoma cell lines. Oncogene 11(9): 1899–1905, 1995
28. Yoshida M, Furumai R, Nishiyama M, Komatsu Y, Nishino N, Horinouchi S: Histone deacetylase as a new target for cancer chemotherapy. Cancer Chemother Pharmacol (suppl 1): S20–26, 2001
29. Marks PA, Richon VM, Rifkind RA. Histone deacetylase inhibitors: inducers of differentiation or apoptosis of transformed cells. J Natl Cancer Inst 92(15): 1210–1216, 2000

Address for offprints and correspondence: JS Strobl, Department of Biochemistry and Molecular Pharmacology, Robert C Byrd Health Sciences Center, West Virginia University, Morgantown, WV, 26506, USA; *Tel.*: 304-293-7151; *Fax*: 304-293-6854; *E-mail*: jstrobl@hsc.wvu.edu

Myc Protein is Differentially Sensitive to Quinidine in Tumor versus Immortalized Breast Epithelial Cell Lines

Zaroui K. Melkoumian, Anna R. Martirosyan, and Jeannine S. Strobl [1]
Department of Biochemistry and Molecular Pharmacology
West Virginia University
Morgantown, West Virginia 26506

Corresponding Author
Jeannine S. Strobl, Ph.D.
Department of Biochemistry and Molecular Pharmacology
West Virginia University
Morgantown, West Virginia
26506-9142

email: jstrobl@hsc.wvu.edu
Phone: 304-293-7151
FAX: 304-293-6854

Key Words: breast cancer, c-myc, differentiation, E2F, MCF-10A, MCF-7, Rb, quinidine

Abbreviations:
DMEM – Dulbecco's Modified Eagle's Medium
ER – estrogen receptor
FBS – fetal bovine serum
HBSS – Hank's Balanced Salt Solution
HMEC – human mammary epithelial cells
K_{ATP} - ATP-sensitive potassium channel
MAPK – mitogen activated protein kinase
MEGM – mammary epithelium growth medium
PBS – phosphate buffered saline
PRF- phenol red-free
Q - quinidine
Rb – retinoblastoma protein
TBS – Tris-buffered saline
TGFβ1 – transforming growth factor beta-1

Abstract

Quinidine regulates growth and differentiation in human breast tumor cells, but the immortalized mammary epithelial MCF-10A cell line is insensitive to quinidine. We found that a morphologically similar differentiation response was evoked by quinidine and c-*myc* antisense oligonucleotides in MCF-7 cells, and this prompted us to investigate the actions of quinidine on c-*myc* gene expression. Myc protein levels were suppressed in human breast tumor cell lines, but not in MCF-10A cells, an observation that supports the hypothesis that suppression of c-*myc* gene expression is involved in the preferential growth and differentiation response of breast tumor cells to quinidine. Quinidine reduced c-*myc* mRNA levels in MCF-7 cells. Acute induction of c-*myc* mRNA by estradiol, as well as the c-*myc* response to sub-cultivation in fresh serum and H-*ras* driven elevations in c-*myc* mRNA were depressed by 50-60% in the presence of quinidine. Quinidine decreased c-*myc* promoter activity in MCF-7 cells in a transient reporter gene assay, and a 168 bp region of human c-*myc* promoter (-100 to +68 with respect to the P1 promoter) was sufficient to confer responsiveness to quinidine. Quinidine is a potential lead compound for developing pharmacological agents to regulate Myc. In addition, the study of quinidine-regulated events is a promising approach to unravel differentiation control pathways that become disrupted in breast cancer.

Introduction

The present work investigates the actions of quinidine on Myc expression in breast epithelial cells. Quinidine, a natural alkaloid, was first used therapeutically as an anti-malarial, and only later, its effectiveness in the suppression of cardiac arrhythmia was discovered. The response of cardiac muscle to quinidine is caused by the blockade of sodium and potassium ion channels however, the basis for quinidine's action on the malarial parasite is unknown (1). The anti-proliferative activity of quinidine in human breast cancer cells *in vitro* was first established in our laboratory. MCF-7, MCF-7*ras*, MDA-MB-231, MDA-MB-435, and T47D human breast cancer cell lines were growth arrested and exhibited a differentiation response to quinidine (2). A number of approaches have been taken to elucidate the mechanism of action of quinidine in human breast epithelium (2,3,4). Disruption of potassium ion permeability as a result of blockade of the plasma membrane ATP-sensitive potassium channels (K_{ATP}) is hypothesized to control cell cycle progression in MCF-7 cells by preventing cell transit from G1 into S phase (4,5). Within 12-24 hours, the profile of G1 regulatory proteins in MCF-7 cells was typical of a G1-arrested condition. The p21/WAF1 protein, an inhibitor of cyclin-dependent kinases 4 and 6 was increased. Total retinoblastoma protein, Rb was suppressed and the hypophosphorylated Rb form was prominent. After several days in quinidine, cells showed evidence of cellular differentiation. The current studies address the changes in c-*myc* gene expression that accompany the anti-proliferative actions of quinidine in human breast epithelial cells. Down-regulation of c-*myc* occurred in MCF-7 tumor cells but not in the immortalized breast epithelial cell line, MCF-10A. We used

quinidine as a chemical probe to explore the pathways involved in the differential regulation of Myc in these two cell lines.

C-myc is a protooncogene whose gene product has a regulatory role in cell cycle progression, cell differentiation, and apoptosis (6,7). Aberrant expression of *c-myc* is very common in breast cancers (8), suggesting its importance in the genesis and/or progression of breast cancer. It has been demonstrated that *c-myc* expression is critical for the growth of both ER-positive and ER-negative breast cancer cells *in vitro* as well as for tumor growth *in vivo* (9). *c-myc* mRNA induction occurs within 20 min after addition of estradiol to quiescent MCF-7 human breast cancer cells (10). In the complex with its dimerization partner, Max, Myc then act as a transcription factor to activate/suppress the expression of its target genes involved in the regulation of cell cycle progression and proliferation. Some of the *c-myc* target genes include *cdc25A, p15Ink4b, p19ARF, gadd 45, odc, cad, p53, cyclin D1,* and *E2F* (11,12). Reversible control of mammary epithelial cell proliferation is possible by the turn-on and turn-off of Myc protein production using a tetracycline-inducible Myc expression system (13). Studies in different cell lines have shown that down-regulation of *c-myc* by antisense oligonucleotides or expression of dominant negative *c-myc* gene accompanies terminal differentiation and permanent withdrawal from the cell cycle (14-18). Collectively, these studies suggest that Myc is an appropriate pharmacologic target for breast cancer intervention.

Materials and Methods

Tissue culture. MCF-7 cells passage #40-50, MCF-7*ras* (19), MDA-MB-231, and MDA-MB-435 cells were maintained in Dulbecco's modified Eagle's medium (DMEM) (BioWhittaker, Walkersville, MD) supplemented with 10% heat-inactivated fetal bovine serum (FBS) (HyClone Laboratories, Inc, Logan, Utah), 2 mM glutamine, and 40 μg/ml gentamicin. MDA-MB-468 (ATCC) cells were grown in 50:50 DMEM/F-12 medium (Invitrogen, Carlsbad, CA). Phenol-red free (PRF) DMEM was obtained from BioWhittaker, Walkersville, MD. Most experiments were performed in DMEM supplemented with 5% FBS. To study the effects of quinidine on estradiol induction of c-*myc,* cells were subcultivated into PRF-DMEM containing 2% charcoal-stripped FBS and subjected to several exchanges of the media to strip cells of endogenous estrogens (20,21). Normal human mammary epithelial cells, HMEC, (Clonetics, San Diego, CA) and MCF-10A (ATCC) were grown in MEGM according to the directions from suppliers. HMEC were grown from frozen stocks and used for 1-3 passages only. The cells were maintained at 37 °C in a humidified atmosphere of 94% air, 6% CO_2. Cells were passaged every 5-6 days (about 70-80% confluent) at ratios of 1:5 (MCF-7, MDA-MB-468) or 1:10 (MCF-7*ras*, MDA-MB-231, MDA-MB-435, and MCF-10A). All cell counts were performed using a hemocytometer and 0.02% Trypan blue to assess cell viability.

Chemicals: Quinidine-HCl (Q) was purchased from Sigma Chemical Co. (St. Louis, MO). Concentrated stock solutions (10mM) were prepared fresh for use by dissolving in sterile water. Estradiol-17β (Steraloids, Wilton, NH) was dissolved in 95% ethanol at a concentration of 2mM and diluted $1:10^6$ in the medium to a final concentration of 2nM.

Transforming growth factor-beta (TGFβ1, T) (R&D Systems, Minneapolis, MN) stock solution (2.5μg/ml) was prepared in 4mM HCl, 1mg/ml BSA and stored at -20°C.

Plasmids: The human *c-myc* probe used for Northern blots was a 9 kb *EcoR*1-*Hind* III genomic fragment spanning exons I and II and intron I isolated from the plasmid pHSR-1 obtained from the American Type Culture Collection (22). The reporter plasmids containing different regions of the human *c-myc* promoter (Del-1, Del-2, Del-4, Frag-E) linked to the firefly luciferase gene were kindly provided by Dr. Bert Vogelstein, Johns Hopkins University (23). The promoterless luciferase plasmid was constructed by deleting the *c-myc* promoter region from the Del-4 plasmid using *Pvu* II restriction enzyme. The human *cyclin D1*- luciferase plasmid (1745CD1-Luc) was kindly provided by Dr. Richard Pestell (The Albert Einstein College of Medicine, Bronx, NY) (24). The E2F-TA-Luc plasmid and control plasmid, TA-Luc, were purchased from Clontech Laboratories, Inc. (Palo Alto, CA).

Oligonucleotide Transfections: c-Myc antisense (5'-AACGTTGAGGGGCAT-3') and sense oligonucleotides (5'-ATGCCCCTCAACGTT-3') were purchased from Sigma-Genosys (Woodlands, TX) and diluted in sterile water to yield concentrated stock solutions of 175 μM. The stock solutions were stored at -20°C for 2 months. Cells were plated at the density of 2.2 x 10^5/35 mm^2 dish on glass cover slips in DMEM/5%FBS. Cells were allowed to attach to the cover slips and then the medium was exchanged to DMEM/2%FBS +/- 9 μM *c-myc* antisense oligonucleotides or 9 μM of *c-myc* sense oligonucleotides as the negative control.

Antibodies: Myc (9E10, sc-40),β-catenin (E-5, sc-7963), Sp1 (PEP2), Sp3 (D-20), and E2F-1 (KH 95), antibodies (Santa Cruz Biotechnology, Santa Cruz, CA) were used at a

dilution as recommended by the supplier. Another E2F-1 antibody (KH 20 + KH 95) directed against two regions of the Rb binding pocket was purchased from Upstate Biotechnology (Lake Placid, NY). Rb (clone G3-245) antibody that recognizes phosphorylated and non-phosphorylated forms was purchased from Pharmingen (San Diego, CA), and a phospho Rb-specific antibody (Ser $^{807/811}$) was purchased from Cell Signaling Technology. Peroxidase-conjugated secondary antibodies were used, and signals were visualized using Super Signal (Pierce, Rockford, IL) or LumiGlo (Cell Signaling Technology, Beverly, MA).

Oil-Red O assay: Cells were plated in 35 mm^2 tissue culture dishes on sterile glass cover slips in DMEM/5%FBS +/- quinidine. After treatment, the cells were fixed (10% formaldehyde and 0.2% calcium acetate in PBS) for 3 minutes and stained with fresh Oil-Red O working solution (Oil-Red O stock solution [0.5% Oil-Red O in 98% Isopropanol] diluted in distilled water in a 3:2 ratio) for 10 minutes. Cells were rinsed in water and counterstained with Mayer's hematoxylin to visualize the cell nuclei. The images were obtained using an Ortholux microscope (Ernst Leitz Wetzlar, Germany) (40x objective), and the data quantified using Image-Pro Plus software (Media Cybenetics, Silver Spring, MD).

Cell cycle analysis: Cell cycle analysis was performed after propidium iodide staining (25) using a FACScan (Becton Dickinson, San Jose, CA) and CellFIT software.

Western blots: Cells were rinsed with 1x PBS (phosphate buffered saline: 137 mM NaCl, 2.7 mM KCl, 4.3 mM Na_2HPO_4 x $7H_2O$, 1.4 mM KH_2PO_4, pH 7.3) and harvested by scraping in boiling lysis buffer (1% SDS, 10 mM Tris, pH 7.4). After boiling for 5 minutes, the cell extract was the supernatant obtained after centrifugation in an

Eppendorf microfuge (14,000 x g, 5 minutes, 4C). Twenty μl aliquots were removed for determination of protein concentrations (BCA assay, Pierce Company). To the remaining extracts, 1 mM DTT and protease inhibitors were added to the final concentrations indicated: PMSF (phenylmethylsulfonyl fluoride, 0.1 mM), aprotinin (1 μg/ml), and leupeptin (1 μg/ml). Cell extract proteins were diluted in sample buffer and denatured by heating at 100 °C for 3 minutes immediately prior to loading onto 10% polyacrylamide gels. Proteins were separated and transferred to PVDF (polyvinylidene difluoride) membranes (Invitrogen, Bethesda, MD). Autoradiographic signals were quantified by densitomery (Personal Densitometer SI, Molecular Dynamics, Sunnyvale, CA) and Image QuaNT software, version 4.1. Myc signals were normalized to the 97 kDa β-catenin protein signals.

Northern blots: Total cellular RNA was purified by the method of Chomczynski and Sacchi (26). Fifteen μg of RNA for each sample were separated on 1.2% agarose-1.9 % formaldehyde gels in MOPS running buffer (20 mM MOPS, 5 mM sodium acetate, 0.5 mM EDTA, pH 8.0), and transferred to 0.2 mμ nitrocellulose paper (Schleicher and Schuell, Keene, NH) by capillary action. Pre-hybridization (15-20 h) and hybridization reactions (40-42 h) were performed in the Micro-hybridization oven (Bellco Glass Inc., Vineland, NJ) at 42 °C for 15-20 h. Hybridization solution included 1.5-2 x 10^6 cpm/ml of denatured *c-myc* DNA fragment labeled with [αP^{32}]dCTP by random priming (Rediprime DNA labeling kit, Amersham Corp., Arlington Hts., IL). The blots were washed in 2x SSC (Standard Saline Citrate)-0.1% SDS twice for 20 minutes each at 37°C. A high stringency wash of the *c-myc* probe was performed for 15 minutes at 42°C in 0.1x SSC-0.1% SDS buffer. The hybridization signals were quantified using PSI-PC

(Molecular Dynamics, Sunnyvale, CA) and ImageQuaNT software, version 4.1. Hybridization signals were normalized to levels of 18S or 28S RNA in the ethidium bromide stained gels.

Reporter gene assay: Confluent MCF-7 cells were re-seeded at a density of $8x10^5/60$ mm^2 dish in 5 ml DMEM/5%FBS. After 20-24 h, when cells were 40-50% confluent, the cell monolayers were rinsed with 1xHBSS buffer (5.4 mM KCl, 108 mM NaCl, 0.34 mM Na_2HPO_4 x $7H_2O$, 4.2 mM $NaHCO_3$, 0.44 mM KH_2PO_4, pH 7.2) and 5ml of DMEM/2%FBS were added. One hour later, transfection mixes containing 5 μg of plasmid DNA in DOTAP transfection reagent (Roche Molecular Biochemicals) were added to the cells. Transfections were terminated 6-7 h later by exchanging the medium with fresh medium +/- quinidine. Cells were harvested 24 h later by scraping into ice-cold lysis buffer (25 mM Tris-phosphate, pH 7.8, 1% Triton X-100, 2mM EDTA, 10% Glycerol). Supernatants from the cell lysates were obtained by centrifugation in an Eppendorf microfuge (14,000 x g, 5 minutes, 4C). Aliquots (20 μl) were removed for protein determinations using the BCA assay. To measure luciferase activity, 50 μl of cell extracts were added to 250 μl of ice-cold luciferase sample buffer (25 mM glycylglycyl, pH 7.8, 15 mM $MgSO_4$) in polypropylene tubes. The samples were warmed to 25 °C. Luciferase activity was measured using an Auto Luminat (LB 953, EG and G-Bertholdt) equipped with a dual injection system for the addition of ATP and luciferin. The relative luciferase units obtained from 50 μl of cell extracts were normalized to 200 μg of cellular proteins. Light generation from purified luciferase (Sigma) was used as the standard in each experiment to ensure that all determinations were performed under linear assay conditions.

Statistics. *SigmaPlot* software (SPSS Inc., Chicago, IL), version 5.0 and *JMP* software (SAS Institute, Inc., Cary, NC) were used for statistical analysis. One way analysis of variance (ANOVA) followed by the Dunnett's test for comparison of multiple groups with control or the Tukey-Kramer test for comparison between the different groups was used. A significance level of 0.05 was used.

Results

Cellular differentiation of MCF-7 cells in response to c-myc antisense oligonucleotides and quinidine.

Lipid droplets are found in the cytoplasm of normal mammary epithelium, and induction of differentiation in human breast cancer cell lines by retinoic acid (27,28), vitamin D analog, 1-α- hydroxyvitamin D5 (29), and oncostatin M (30) is marked by the accumulation of cytoplasmic lipid droplets. Quinidine (90 μM) promoted the appearance of a more differentiated phenotype in MCF-7 cells characterized by an enlarged cytoplasm, rearrangement of the cytokeratin 18 cytoskeleton, and the accumulation of cytoplasmic lipid droplets (2). Figure 1 summarizes a series of experiments in which differentiation in human mammary cells *in vitro* in response to either quinidine (90 μM) or c-*myc* antisense or sense oligonucleotides was evaluated by Oil Red O staining of cytoplasmic lipid droplets. Only normal human mammary epithelial cells (HMEC) showed cytoplasmic lipid droplets in control, untreated cultures. HMEC exposed to quinidine (90 μM) for 72 h showed no increase in lipid droplet accumulation, and no signs of cytotoxicity. The latter observation was consistent with an earlier report that indicated quinidine did not inhibit HMEC proliferation (2). However, HMEC barely proliferate. In a 10-day growth experiment, the HMEC doubled over a period of ~120 h, and then remained at a stable cell number for another 5 days (in the presence or absence of 90 μM quinidine). MCF-10A cells are immortalized human mammary epithelial cells that do not form tumors in animals (31). However, MCF-10A cells proliferate more rapidly in culture (doubling time 37 h) than the early passage MCF-7 cells used in these experiments (doubling time 57 h). MCF-10A cells provide one test for discriminating

whether quinidine acts upon all cells with a rapid proliferation rate, or whether quinidine differentially affects tumorigenic mammary epithelial cells. Control MCF-10A cells did not accumulate cytoplasmic lipid droplets, and neither quinidine treatment or c-*myc* antisense oligonucleotides elicited this response (data not shown). In contrast, lipid droplet accumulation and cytoplasmic enlargement was evident in MCF-7 cells treated with 90 μM quinidine for 72 h and with c-*myc* antisense for 96 h. Control (untreated) MCF-7 cells and MCF-7 cells exposed to c-*myc* sense oligonucleotides for 96 h did not accumulate lipid droplets. We conclude that quinidine and c-*myc* antisense oligonucleotides promote a more differentiated phenotype in MCF-7 cells. Quinidine promoted lipid droplet accumulation in MDA-MB-231, MDA-MB-435, MCF-7*ras* and T47D cells (2) suggesting that this differentiation response is common among human mammary tumor cell lines.

Quinidine suppresses Myc induction and cell growth in human breast cancer cells in vitro, but not that of non-tumorigenic mammary epithelial cells.

Transient induction of *c-myc* mRNA and protein occurs 20-30 minutes after mitogenic stimulation of quiescent MCF-7 human breast cancer cells (10). We tested whether quinidine affected Myc protein induction following release of MCF-7 cells from confluency into medium containing fresh serum. MCF-7 cells were grown in tissue culture flasks until 90-95 % confluent to obtain cell populations that were 85% G0/G1 phase (4). These confluent cells were then sub-cultivated into the medium containing fresh serum (5%) plus 90 μM quinidine or H_2O (vehicle). Myc protein levels were measured at the times indicated (Figure 2). A maximal 15-fold induction of Myc protein occurred 90 minutes after sub-cultivation. The response is transient and Myc protein

levels returned to baseline by 3 hours. Quinidine suppressed the rise in Myc protein, with a maximal 60% inhibition observed at 60 minutes.

Myc is a target for ubiquitination and degradation through the proteasome pathway (32). The proteasome inhibitor, MG-132 did not preserve Myc protein levels in quinidine-treated cells (data not shown) suggesting that quinidine does not inhibit Myc levels by stimulating Myc degradation.

Quinidine also suppressed Myc expression that was stimulated in response to sub-cultivation in other breast tumor cell lines (Figure 3, hatched bars): MCF-7*ras* (by 82 %), MDA-MB-231 (by 66%), MDA-MB-435 (by 59%). The degree of suppression of Myc protein levels by quinidine correlated well with the extent of inhibition of proliferation in each of these cell lines (Figure 3, solid bars). MCF-10A is a rapidly proliferating but non-tumorigenic mammary epithelial cell line that expresses high Myc protein levels. In contrast to the tumor cell lines, quinidine had no effect on Myc protein expression or proliferation of MCF-10A cells (Figure 3). These results demonstrate the ability of quinidine to selectively inhibit growth and Myc protein in tumorigenic breast cells but not in an immortalized, non-tumorigenic breast epithelial line.

Suppression of Myc protein and growth arrest by quinidine is not mediated through TGF-β1 response pathways.

Transforming growth factor β-1 (TGF-β1) regulates epithelial cell growth, differentiation, adhesion, movement, and death, but most mammary tumor cell lines are resistant to the growth inhibitory effects of TGF-β1, due to defects or deficiencies in TGF-β1 receptors or the TGF-β1 signaling pathway. C-*myc* is an important target of

TGF-β1 (33,34). In MCF-10A cells, TGF-β1 stimulates the formation of an inhibitory complex on the c-*myc* promoter and rapid down-regulation of *c-myc* mRNA, but this response is lost from MCF-10A cells after transformation with c-Ha-*ras* and c-*erb*B2 oncogenes (35). TGF-β1 resistant MDA-MB-468 breast tumor cells lack Smad4, a transcription factor and an essential TGFβ1 signaling molecule (35). In MDA-231 cells, resistance to TGFβ is not fully understood, however, ectopic expression of TGF-β type III receptor suppressed tumorigenicity of MDA-MB-231 cells (36). In contrast, MCF-7 cells have a partial response to TGFβ growth inhibition, and ectopic TGFβRIII restores autocrine TGF-β1 activity in MCF-7 cells (37). Despite these distinct defects in TGFβ1 signaling, quinidine inhibited proliferation in all breast tumor cell lines tested, implying that quinidine acts independently of TGF-β1 pathways (Figure 4A). Furthermore, quinidine had no effect on the growth of MCF-10A cells (Figure 3) in which the TGF-β1 pathway is intact. This result is important because it argues against the possibilities that quinidine acts either to restore a TGF-β1 response network, or to compensate for TGF-β1 defects. In Figure 4, the effects of quinidine and TGF-β1 on proliferation and Myc protein levels in a single experiment is summarized. We found (Figure 4A) in this experiment that after 72 hours in quinidine MCF-10A cell numbers decreased slightly (24%), TGF-β1 alone caused a 54% reduction in cell numbers, and that the combination quinidine plus TGFβ1 appeared to have an additive effect, reducing overall cell numbers by 71%. Similar reductions in the level of Myc protein in MCF-10A cells by quinidine (17%), TGF-β1 (54%), and the combination (Q+T, 71%) were observed (Figure 4B). The data support the hypothesis that quinidine and TGF-β1 act through independent mechanisms to reduce c-*myc* expression and cell proliferation.

Quinidine suppresses acute induction of c-myc mRNA and S phase progression by estradiol.

Acute induction of *c-myc* mRNA transcription in MCF-7 cells exposed to estradiol is critical to progression through G1 phase of the cell cycle and the proliferative response to estradiol (10,38). At one hour, quinidine suppressed estradiol-induced *c-myc* mRNA levels in MCF-7 cells in a concentration dependent fashion. Maximum inhibition (60%) of c-*myc* mRNA was achieved with 90 μM quinidine (Figure 5A). These results are in good agreement with 60% suppression of Myc protein at one hour by 90 uM quinidine following cell sub-cultivation into fresh serum (Figure 2). We conclude that inducible *myc* gene expression is suppressed but not completely inhibited by quinidine. Despite incomplete suppression of Myc, the actions of 90 μM quinidine were sufficient to inhibit estradiol stimulated MCF-7 cell cycle progression into S phase (Figure 5B). Confluent cells (80-85% G0/G1) were sub-cultivated into PRF-DMEM + 2% stripped FBS; 30 hours after plating, only 11% of the control cells progressed into the S phase. Estradiol (2nM) stimulated 34% of the cells to enter into S phase by 30 hours, and this response was nearly completely blocked in the presence of quinidine (14% S phase cells).

Quinidine suppresses basal and H-ras-driven c-myc mRNA and protein expression.

In MCF-7 cells, Myc is transiently induced during the G0-G1 phase transition and then remains at a constant low level throughout the cell cycle (7). To ascertain whether quinidine affected basal *c-myc* expression, MCF-7 cells were incubated for 24 hours with 30 or 90 μM quinidine. A twenty-four hour treatment with 30 μM quinidine reduced Myc protein (Figure 6A) and mRNA (Figure 6B) levels by approximately 50%, and 90 μM

quinidine had a more pronounced effect upon basal Myc protein and mRNA levels. MCF-7 cells stably transfected with H-*ras* (MCF-7*ras)* have an activated *ras* signaling pathway and express higher levels of Myc protein and mRNA than wild-type MCF-7 cells. Quinidine reduced Myc protein and mRNA expression in MCF-7*ras* cells to that seen in wild-type MCF-7 cells exposed to quinidine, suggesting that quinidine interferes with H-*ras* activated pathways that stimulate Myc. Collectively, our data demonstrate quinidine inhibits basal c-*myc* expression, estradiol-inducible c-*myc* expression, c-*myc* expression stimulated by sub-cultivation, and H-*ras*-driven c-*myc* expression in MCF-7 human breast tumor cells.

Quinidine inhibits c-myc promoter activity.

The ability of quinidine to inhibit c-*myc* promoter activity was tested using myc-luciferase reporter plasmids transiently transfected into MCF-7 cells. Cells were incubated in the presence of quinidine for 24 hours following transfection, and luciferase activity was measured in the cell extracts. Luciferase activity in mock-transfected cells was less than 0.1% of the activity in control cells transfected with Del-1 (Figure 7A). Quinidine treatment caused a concentration-dependent decrease in the activity of the Del-1 *c-myc* promoter. Ninety μM quinidine decreased *c-myc* promoter activity by 60%, similar to the observed levels of inhibition of Myc protein and mRNA.

To better define the region of the *c-myc* promoter responsive to quinidine, a series of 5'-deletion mutants of Del-1 was tested (Figure 7B). The *cyclin D1*-luciferase (CD1) and promoterless luciferase (Luc) plasmids were used as controls. Relative luciferase activity driven by the various plasmids was compared with Del-1. Quinidine suppressed the

activity of all the *myc* 5'deletion mutants by 60-70%, but had a minimal effect on luciferase expression driven by the *cyclinD1* promoter, suggesting that the effect of quinidine is promoter specific and not related to more general effects associated with cell cycle arrest in G1. Quinidine did not inhibit the enzymatic activity of the purified luciferase protein (data not shown). We conclude that quinidine suppresses the activity of the *c-myc* promoter, and that a 168 bp region of human c-myc promoter from -100 to +68 with respect to the P1 promoter is sufficient to confer responsiveness to quinidine.

Although quinidine does not appear to act by restoring TGFβ1 pathways that suppress Myc production, the TCE, a TGF-β1 control element, -86 bp to –63 bp with respect to P1, that was first identified in keratinocytes, is present in the quinidine responsive region of the c-*myc* promoter (39). This element controls repression of the c-*myc* promoter by Rb, and this might be important to the quinidine response.

The actions of quinidine on the c-*myc* Del-4 promoter and the cyclin D1 (CD1) promoter were compared in MCF-10A and MCF-7 cells. The cyclin D1 promoter was active in MCF-10A cells (877 cpm ± 23, mean ± range of duplicates in n=2 experiments) and was not regulated by quinidine (90 μM, 24 h) (894 cpm ± 23, n = 2). The c-*myc* Del-4 promoter, the most active of the c-*myc* promoter constructs in MCF-7 cells, was completely inactive in MCF-10A cells in 3 of 4 experiments. This was not an experimental artifact, because two of these experiments showed excellent activity of the cyclin D1 promoter in the MCF-10A cells, and this same Del-4 construct was active in MCF-7 cells transfected in parallel with the MCF-10A cells. This result suggested that the cis-acting elements required for transcription of the *myc* gene differ in MCF-10A and MCF-7 cells.

Quinidine differentially regulates Rb/E2F1 in MCF-7 and MCF-10A cells

E2F transcription factors drive G1-S progression by activating the expression of genes required for entry into S phase (40,41). Two E2F consensus DNA binding sites are located between P1and P2 of the c-*myc* promoter, and participate in the activation of c-*myc* transcription by E2F family members. These sites are present in Del-4 (-348 *myc)*, and might contribute to its strong promoter activity in MCF-7 cells. E2F1 protein levels were reduced by 54% in MCF-7 cells exposed to 90 μM quinidine for 24 h (Figures 8 and 9), and total E2F transcriptional activity measured using an E2F-driven luciferase reporter gene decreased by 82 ± 2% (mean ±SE, n=3). Quinidine did not affect protein levels of two other c-*myc* transcriptional activators, Sp1 and Sp3 (42), either at 4 h or 24 h (Figure 8). The results suggest that decreased E2F activity contributed to the suppression of c-*myc* promoter activity as well as Myc protein levels observed in MCF-7 cells exposed to quinidine for 24 hours. However, there was no decrease in E2F1 protein in MCF-7 cells after a 4 h incubation with 90 μM quinidine (data not shown), implying that quinidine inhibition of early myc mRNA and protein induction (Figures 2 & 5) occurred by a different mechanism. Nevertheless, Myc acts a positive regulator of E2F protein levels (43). Therefore, suppression of early Myc expression by quinidine might contribute to the fall in E2F1 levels that occurred by 24 h.

Hypophosphorylated Rb protein regulates E2F transcriptional activity by sequestering E2F in an inactive state in the Rb binding pocket. Using antibodies that recognize total Rb or only the phosphorylated form of Rb (Ser $^{807/811}$) we showed that quinidine-treated MCF-7 cells were relatively depleted of phosphorylated Rb (Figures 8 and 9). Immunoprecipitation of total Rb confirmed the presence of increased E2F1 bound to Rb

after quinidine treatment compared with control MCF-7 cells (data not shown). Thus, quinidine acts via at least two mechanisms to reduce levels of free E2F1 protein resulting in suppression of E2F-mediated gene activation.

E2F1, Sp1 and Sp3 protein levels were lower in MCF-10A cells than in MCF-7 cells and did not change with quinidine (90 μM, 24 h) treatment (Figures 8 and 9). Rb protein phosphorylation levels were nearly identical in control and in quinidine treated MCF-10A cells. These observations support the hypothesis that quinidine regulation of E2F1 in MCF-7 cells is critical to its actions on growth and Myc expression. In addition, MCF-10A cells expressed a unique E2F1 immunoreactive protein, which we refer to as truncated, or tE2F1 (Figure 8). This 30 kDa protein bound E2F1 antibodies from two commercial sources highly specifically. The monoclonal antibodies that were used recognize two regions within the E2F1 Rb binding domain, and we conclude that MCF-10A cells express a truncated, E2F1-like protein that retains the Rb binding domain. This protein appears to be transcriptionally inactive. We could not detect luciferase activity in MCF-10A cells transfected with the E2F driven-luciferase reporter gene (data not shown) using as a positive control for the transfection assays, the cyclin D1-driven luciferase reporter gene. Collectively, our results suggest that the 55 kDa E2F-1 plays a minor role in driving proliferation in MCF-10A cells. This idea merits more rigorous examination, however the observed quinidine resistance of MCF-10A cells fits well the model that quinidine inhibition of E2F-1 transcriptional activity is important for its antiproliferative action and suppression of Myc expression.

Discussion

In the present study, we demonstrated that pharmacological inhibition of mammary epithelial tumor cell proliferation by quinidine was closely associated with reduced Myc protein expression. Quinidine reduced Myc expression by 50-70% at all levels of investigation including protein, mRNA and c-*myc* promoter activity in MCF-7 cells. Given the importance of Myc to cell survival and growth, and the redundancy built into signaling pathways that control these processes, quinidine is a remarkably effective Myc expression inhibitor. Quinidine interfered with estrogen-inducible *myc* expression, *ras*-MAPK pathways stimulating *myc*, and mechanisms invoked by the release of cells from confluency into fresh serum leading to myc activation all of which are likely to engage components of growth factor signaling pathways.

The cdk/Rb/E2F pathway plays a critical role in G1 cell cycle progression and cellular differentiation (40, 41). Rb regulates levels of free E2F transcription factors. Unphosphorylated Rb acts as a tumor suppressor protein and sequesters E2F proteins in a transcriptionally inactive state by binding them in the Rb binding pocket. Phosphorylation of Rb or the binding of certain oncogenic viral proteins to this binding pocket, causes the release of E2F1, 2, and 3 and triggers G1-S cell cycle progression. Our results showed that after 24 hours in quinidine MCF-7 cells exhibit an overall suppression in the activity of the cdk/Rb/E2F pathway. Eighty percent of MCF-7 cells were arrested in G1/G0 phase of the cell cycle (3,4). Protein levels of cdk4 and cyclin D1 were reduced and levels of the cyclin-dependent kinase inhibitor, p21/WAF1, were increased favoring the retention of retinoblastoma protein in its hypophosphorylated, tumor suppressor state (2). Myc expression and that of a Myc target protein, E2F1, were

suppressed, but levels of the transcription factors, Sp1 and Sp3, were unaffected by quinidine treatment. E2F activated transcription was decreased by 82% in MCF-7 cells incubated with quinidine for 24 h. We conclude that suppression of E2F transcriptional activity is an important mechanism of quinidine action.

We also propose the idea that hypophosphorylated retinoblastoma is an important mediator of the response to quinidine. Hypophosphorylated Rb is a transcriptional repressor of myc. The activity of the human c-myc promoter was inhibited by quinidine in transiently transfected MCF-7 cells, and the quinidine responsive region, –100 to +68 bp, contains the Rb responsive region. Quinidine did not promote the differentiation of MDA –MB-468 human breast tumor cells that lack Rb protein (Strobl, unpublished), and the reintroduction of Rb into Rb-/- SAOS cells, elicited a large cytoplasm phenotype remarkably similar to that seen in quinidine-treated MCF-7 cells (44).

The acute rise in Myc that occurred 90 minutes after exposure to estradiol or subculturing in fresh serum, was suppressed by quinidine independently of its actions upon E2F1 or Rb. E2F1, Sp1 and Sp3 proteins levels did not change during a 4 h incubation of MCF-7 cells with quinidine, and the appearance of hypophosphorylated Rb in quinidine-treated MCF-7 cells occurred between 12 and 24 h (2). Ionic changes elicited by quinidine might attenuate the rapid induction of c-*myc* in MCF-7 cells. In lymphocytes, a rapid induction of c-*myc* gene expression was initiated in response to stimuli that raised intracellular Ca^{+2} (45), and pharmacological inhibition of potassium channels prevented the rise in intracellular Ca^{+2} in many cell systems (46). Quinidine blocked potassium channels in MCF-7 cells at concentrations that antagonize c-*myc* induction in MCF-7 cells, causing membrane depolarization within 3 minutes (3,4).

Membrane depolarization can alter intracellular Ca^{+2} by reducing the driving force for calcium entry through non-selective cation channels (46). In addition, quinidine has been reported to inhibit inositol 1,4,5-trisphosphate binding to its receptor thereby blocking Ca^{+2} release from intracellular stores (47).

MCF-10A cells continued to proliferate in the presence of quinidine, and Myc protein levels were not significantly reduced. In comparison with MCF-7 cells, MCF-10A cells maintained high levels of phosphorylated Rb expression in the presence of quinidine. MCF-10A cells also failed to differentiate in response to treatment with either quinidine or c-*myc* antisense oligonucleotides, and these results are consistent with the hypothesis that both hypophosphorylated Rb and reduced Myc expression are required for the Oil Red O differentiation response in mammary epithelial cells.

MCF-10A cells showed evidence of a highly expressed 30 kDa immunoreactive E2F1-like protein. MCF-10A cells expressed extremely low levels of 55 kDa E2F1 protein. We could not demonstrate transcriptional activation of an E2F-driven luciferase reporter gene in MCF-10A cells, and in gel mobility shift assays using extracts of MCF-10A cells, Botos *et al.*, could find no evidence for the presence of E2F1 binding to the DNA consensus sequence for E2F (48). We conclude that MCF-10A cells over express a 30kDa protein that retains a Rb binding domain, but lacks E2F DNA binding and transcriptional activity. The binding of a truncated E2F1-like protein to hypophosphorylated Rb could competitively inhibit the binding of other Rb pocket protein binding partners and/or interfere with the ability of hypophosphorylated Rb to promote differentiation. The altered E2F-1/Rb pathway in MCF-10A cells is a likely explanation for their resistance to quinidine actions on Myc and cell differentiation.

Acknowledgements

The authors are grateful to Dr. Bert Vogelstein, Johns Hopkins University and Dr. Richard Pestell, Albert Einstein College of Medicine for providing myc-luciferase and cyclin D1-luciferase constructs, respectively. This work was supported by grants DAMD 17-99-1-9447 and DAMD 17-00-1-500 from the US Department of Defense Breast Cancer Research Program.

Legends

Figure 1. Cellular differentiation of MCF-7 cells in response to c-myc antisense oligonucleotides and quinidine.
Oil Red O staining of MCF-7 cells treated with nothing (A and D), 90 uM quinidine for 72 (B) or 120 (C) hours, *c-myc* antisense (E) or sense (F) oligonucleotides for 96 hours. Oil Red O staining of normal human mammary epithelial cells, HMEC, control (G) or treated with 90 uM quinidine (H) for 72 hours. Cells were counterstained with hematoxylin to visualize the cell nuclei (blue color).

Figure 2. Quinidine suppresses Myc protein induction in MCF-7 cells.
Confluent (Cf) MCF-7 cells were sub-cultivated at 0 time in DMEM/5%FBS (solid bars) or in DMEM/5%FBS containing 90 μM quinidine (hatched bars). Cells were harvested for Western blot analysis at the times indicated. Myc protein signals were quantified by densitometry and normalized to the β-catenin signals. Data shown in the bar graph are the mean Myc protein signals +/- S.D. of n =3 experiments expressed as a percent of maximal stimulation (at 1.5 hours). The gel scans below the bar graph are a single representative experiment performed with 80 μg of cell extract protein/lane.
* Significantly different from control ($p<0.05$).

Figure 3. Quinidine suppresses Myc induction and cell growth in human breast cancer cells in vitro, but not that of non-tumorigenic mammary epithelial cells.
For the cell count assay (solid bars) confluent cells were sub-cultivated at the density of $1x10^5/35\ mm^2$ dish in DMEM/5%FBS +/- 90 μM quinidine or MEGM (for MCF-10A) +/- 90 μM quinidine and counted 96 hours later using a hemocytometer.
For the Western blot assay (hatched bars) total cellular proteins from control or 90 μM quinidine treated cells were extracted one (MCF-7*ras*, MCF-7, MCF-10A) or two (MDA-MB-231, MDA-MB-435) hours after sub-cultivation of confluent cells into DMEM/5% FBS. Myc protein signals were quantified by densitometry and normalized to the β-catenin signals.

Data are the mean +/- S.D. of n=3 experiments.
* Significantly different from control values ($p<0.05$).

Figure 4. Suppression of Myc protein and growth arrest by quinidine is not mediated by TGF-β1 response pathway.

A. Confluent cells were sub-cultivated in DMEM/5% FBS at the density of $1x10^5$ (MDA-MB-231, MDA-MB-468, MCF-10A) or $2x10^5$ (MCF-7) per 35 mm^2 tissue culture dish in the presence of: C-vehicle (4mM HCl, 1mg/ml BSA - 0.5 μl/ml of medium), Q- 90 μM quinidine, T-5ng/ml TGFβ1, T+Q-90 μM quinidine + 5ng/ml TGFβ1. Cells were harvested 72 or 96 (for MCF-7) hours later and counted using a hemocytometer. The bar graphs show cell numbers as mean +/- SE of n=2 experiments (MCF-7, MDA-MB-231, MDA-MB-435). The MCF-10A data are the mean ± SD or triplicates in a single experiment.

B. Confluent MCF-10A cells were sub-cultivated in MEGM containing C, Q, T, or T+Q as described in A. Total cellular proteins were extracted 24 hours later, and analyzed for Myc and β-catenin by Western blot.

Figure 5. Quinidine suppresses acute induction of *c-myc* mRNA and S phase progression by estradiol.

A. Confluent MCF-7 cells were sub-cultivated in PRF-DMEM/2% stripped serum, and estrogen-depleted for 40 hours. Induction of c-myc mRNA by 2 nM estradiol +/- indicated concentrations of quinidine was measured after 1 hour by isolating total cellular RNA and Northern blotting. c-*myc* mRNA signals were normalized to the 28S ribosomal signal in the ethidium bromide stained gel. Data shown on the bar graph are the mean +/- S.D. of n = 3, except for 30 and 50 μM quinidine that are from a single experiment. Values for E_2 and Q+E_2 treated groups are reported relative to control group (control=1).

B. MCF-7 cells were treated with C-0.01% Ethanol (vehicle), Q- 90 μM quinidine, E_2- 2nM estradiol, Q+E_2- 90 μM quinidine + 2nM E_2. Cell cycle phase distribution was analyzed by flow cytometry 30 hours later. Data are the mean +/- S.D. of n = 4 experiments.
* Significantly different from control cells ($p<0.05$).
# Significantly different from E_2 cells ($p<0.05$).

Figure 6. Quinidine suppresses basal and H-ras-driven *c-myc* mRNA and protein expression.

Confluent MCF-7 (solid bars) and MCF-7*ras* (hatched bars) cells were sub-cultivated into DMEM/5% FBS +/- indicated concentrations of quinidine. Cells were harvested 24 hours later and Myc protein (A) or mRNA (B) levels were analyzed by Western or Northern blots, respectively. Myc protein and mRNA signals were normalized to the β-catenin and 18S ribosomal RNA signals, respectively. Data shown on the bar graphs are the mean +/- S.D. of n= 4 (MCF-7) and n=3 (MCF-7*ras*) experiments for the panel A or n=1 for the panel B.
* Significantly different from control values ($p<0.05$).

Figure 7. Suppression of *c-myc* promoter activity by quinidine.

A. MCF-7 cells were transfected with 5 μg/dish of Del-1 (-2265 myc) *c-myc*-luciferase reporter plasmid or with the transfection mix alone (DOTAP). At the end of transfection cells were

incubated for 24 hours in DMEM/5%FBS + the indicated concentrations of quinidine before preparing cell extracts for luciferase assay. Data shown are the mean luciferase activity +/- S.D. of n =3 experiments (90 and 120μM quinidine) and n=2 experiments (30 and 50μM quinidine). The data are expressed as a percent of luciferase activity in control cells (100%). Luciferase activity in mock-transfected cells (DOTAP) was < 0.01% that of control cells. Luciferase cpm in MCF-7 cell extracts in these experiments were: background (≤ 30), del-1 (200-500) and del-4 (2800-6000).

* Significantly different from control (0 quinidine) cells (p<0.05)

B. Structures of the reporter plasmids. *c-myc* and *cyclin D1* promoter regions are solid;the luciferase coding region is indicated in white. P1 and P2 are the sites of the transcription initiation from the respective *c-myc* promoters. The nucleotide locations of 5' and 3'-ends of the myc-luc constructs are given with respect to the P1.

The effect of quinidine on *c-myc* promoter activity in 5'-deletion mutants is shown to the right of each promoter structure. Cells were transfected with 5 μg/dish of *c-myc*-luc (Del-1, Del-2, Del-4, Frag-E) or *cyclinD1*-luc (CD1) reporter plasmids. At the end of transfection cells were incubated for 24 hours in DMEM/5%FBS +/- 90 uM quinidine before preparing cell extracts for luciferase assay. Luciferase activity driven by Del-1 in the absence of quinidine was set equal to one, and the activity of all the other promoters ± 90 μM quinidine was compared to 1. The percent change in luciferase activity by quinidine for each promoter is indicated.

* Significantly different from control values (p<0.05). Luciferase activity in cells transfected with promoterless construct was less than 2 % of the activity in control cells transfected with Del-1. Data are the mean +/- S.D. of at least n=3 experiments.

Figure 8. Differential actions of quinidine on Rb and E2F1 in MCF-7 and MCF-10A cells. Cells from confluent flasks were sub-cultured in DMEM + 5% FBS ± 90 μM quinidine. Control (C) and quinidine-treated (Q) cells were harvested after 24 h and levels of immunoreactive E2F1, total Rb (T-Rb), phospho ($Ser^{807/811}$)Rb (P-Rb), Sp1 and Sp3 were measured by Western blot. Total protein per lane was identical in MCF-7 and MCF-10A cells: E2F1 (60 μg/lane), T-Rb (80 μg/lane), P-Rb (60 μg/lane), Sp1 (10 μg/lane) and Sp3 (40 μg/lane). Data shown are representative of 2-4 independent experiments.

Figure 9. Phospho($Ser^{807/811}$)Rb and E2F1 are decreased in quinidine-treated MCF-7 cells. Western blot immunoreactive signals corresponding to Total Rb, phosphoRb (p-Rb), and 55kDa E2F1 protein levels obtained from extracts of cells exposed to 90 μM quinidine for 24 h were quantified by densitometry. The value of the control signal for each protein was set to 100% in each experiment. Data shown are the signal in quinidine-treated cells expressed as a fraction of the control. Data shown are the mean ± SE of n=4 experiments for MCF-7 cells and the mean and range of n=2 experiments for E2F1 and Total Rb in MCF-10A cells, and the mean ± SE of n=3 experiments for p-Rb in MCF-10A cells.

References

1. Hondeghem LM, Roden DM In: Basic and Clinical Pharmacology, 8th edition, BG Katzung (Ed.). Lange Medical Publications, NY;2001:219-244.

2. Zhou Q, Melkoumian ZK, Lucktong A, Moniwa M, Davie JR, Strobl JS. Rapid induction of histone hyperacetylation and cellular differentiation in human breast tumor cell lines following degradation of histone deacetylase-1. J Biol Chem 2000;275:35256-35263.

3. Woodfork K, Wonderlin W, Peterson V, Strobl J. Inhibition of ATP-sensitive potassium channels causes reversible cell-cycle arrest of human breast cancer cells in tissue culture. J Cell Physiol 1995; 162:163-171.

4. Wang S, Melkoumian Z, Woodfork K, Cather C, Davidson A, Wonderlin W, Strobl J. Evidence for an early G1 ionic event necessary for cell cycle progression and survival in the MCF-7 human breast carcinoma cell line. J Cell Physiol 1998;176:456-464.

5. Wonderlin WF, Woodfork K, Strobl J. Changes in membrane potential during the progression of MCF-7 human mammary tumor cells through the cell cycle. J Cell Physiology 1995;165:177-185.

6. Amati B, Land H. Myc-Max-Mad: a transcription factor network controling cell cycle progression, differentiation and death. Current Opinion in Genetics and Development 1994;4:102-108.

7. Henriksson M, Luscher B. Proteins of the Myc network: essential regulators of cell growth and differentiation. Adv Cancer Res 1996;68:109-182.

8. Deming SL, Nass SJ, Dickson RB, Trock BJ. C-myc amplification in breast cancer: a meta-analysis of its occurrence and prognostic relevance. Br J Cancer 2000;83:1688-95.

9. Nass SJ, Dickson RB. Defining a role for c-Myc in breast tumorigenesis. Breast Cancer Research and Treatment 1997;44:1-22.

10. Dubik D, Shiu RP. Transcriptional regulation of c-myc oncogene expression by estrogen in hormone-responsive human breast cancer cells. J Biol Chem 1988;263 :12705-12708.

11. Dang CV. C-Myc target genes involved in cell growth, apoptosis, and metabolism. Mol and Cell Biol 1999;18:1-11.

12. Staller P, Peukert K, Kiermaier A, Seoane J, Lukas J, Karsunky H, Moroy T, Bartek J, Massague J, Hanel F, Eiler, M. Repression of p15INK4b expression by Myc through association with Miz-1. Nat Cell Biol 2001;3:392-9.

13. D'Cruz CM, Gunther EJ, Boxer RB, Hartman JL, Sintasath L, Moody SE, Cox JD, Ha SI, Belka GK, Golant A, Cardiff RD, Chodosh LA. c-MYC induces mammary tumorigenesis by means of a preferred pathway involving spontaneous Kras2 mutations. Nat. Med 2001;7:235-239.

14. Ebinuma H, Saito H, Saito Y, Wakabayashi K, Nakamura M, Kurose I, Ishii H. Antisense oligodeoxynucleotide against c-myc mRNA induces differentiation of human hepatocellular carcinoma cells. Int J Oncol 1999;15: 991-999.

15. Canelles M, Delgado MD, Hyland KM, Lerga A, Richard C, Dang CV, Leon J. Max and inhibitory c-Myc mutants induce erythroid differentiation and resistance to apoptosis in human myeloid leukemia cells. Oncogene 1997;14:1315-1327.

16. Griep AE, Wesphal H. Antisense Myc sequences induce differentiation of F9 cells. Proc Natl Acad Sci USA 1988;85: 6806-6810.

17. Holt JT, Redner RL, Neinhuis A W. An oligomer complementry to c-myc mRNA inhibits proliferation of HL-60 promyelocytic cells and induces differentiation. Mol Cell Biol 1988;8: 963-973.

18. Prochownik EV, Kukowska J, and Rodgers C. c-Myc antisense transcripts accelerate differentiation and inhibit G1 progression in murine erythroleukemia cells. Mol Cell Biol 1988;8:3683-3695.

19. Kasid A, Lippman M, Papageorge A, Lowy D,Gelmann E. Transfection of v-ras^{H} DNA into MCF-7 human breast cancer cells bypasses dependence on estrogen for tumorigenesis. Science 1985;228: 745-728.

20. Strobl JS, Kirkwood KL, Lantz TK, Lewine MA, Peterson VA, Worley JF. Inhibition of human breast cancer cell proliferation in tissue culture by the neuroleptic agents pimozide and thioridazine. Cancer Res 1990;50:5399-405.

21. Strobl JS, Lippman ME. Prolonged retention of estradiol by human breast cancer cells in tissue culture. Cancer Res 1979;39:3319-27.

22. Alitalo K, Schwab M, Lin C, Varmus H E, Bishop JM. Homogeneously staining chromosomal regions contain amplified copies of an abundantly expressed cellular oncogene (c-myc) in malignant neuroendocrine cells from a human colon carcinoma. PNAS 1983;89:1707-1711.

23. He TC, Sparks AB, Rago C, Hermeking H, Zawel L, da Costa LT, Morin PJ, Vogelstein B, Kinzler KW. Identification of c-MYC as a target of the APC pathway. Science 1998;281:1509-1512.

24. Albanese C, Johnson J, Watanabe G, Eklund N, Vu D, Arnold A, Pestell RG. Transforming p21ras mutants and c-Ets-2 activate the cyclin D1 promoter through distinguishable regions. J Biol Chem 1995; 270:23589-97.

25. Vindelov L, Christensen I. Detergent and proteolytic enzyme-based techniques for nuclear isolation and DNA content analysis. Methods Cell Biol 1994;41:219-229.

26. Chomczynski P, Sacchi N. Single-step method of RNA isolation by acid guanidium thiocyanate-phenol-chloroform extraction. Anal Biochem 1987;162:156-159.

27. Jing Y, Zhang J, Waxman S, Mira-y-Lopez R. Upregulation of cytokeratins 8 and 18 in human breast cancer T47D cells is retinoid-specific and retinoic acid receptor-dependent. Differentiation 1996;60:109-117.

28. Bacus SS, Kiguchi K, Chin D, King CR, Huberman E. Differentiation of cultured human breast cancer cells (AU-565 and MCF-7) associated with loss of cell surface HER-2/neu antigen. Mol Carcinogen 1990;3:350-362.

29. Mehta RR, Bratescu L, Graves JM, Green A, Mehta RG. Differentiation of human breast carcinoma cells by a novel vitamin D analog: 1alpha-hydroxyvitamin D5. Int J Oncol 2000;16:65-73.

30. Douglas AM, Grant SL, Goss GA, Clouston DR, Sutherland RL, Begley CG. Oncostatin M induces the differentiation of breast cancer cells. Int J Cancer 1998;75:64-73.

31. Giunciuglio D, Culty M, Fassina G, Masiello L, Melchiori A, Paglialunga G, Arand G, Ciardiello F, Basolo F, Thompson EW, et al. Invasive phenotype of MCF10A cells overexpressing c-Ha-ras and c-erbB-2 oncogenes. Int J Cancer 1995;63:815-22.

32. Gross-Mesilaty S, Reinstein E, Bercovich B, Tobias KE, Schwartz AL, Kahana C, Ciechanover A. Basal and human papillomavirus E6 oncoprotein-induced degradation of Myc proteins by the ubiquitin pathway. Proc Natl Acad Sci U S A 1998;95:8058-63.

33. Alexandrow M., Kawabata M., Aakre M., Moses H. Overexpression of the c-Myc oncoprotein blocks the growth-inhibitory response but is required for the mitogenic effects of transforming growth factor beta 1. Proc Natl Acad Sci USA 1995;92:3239-43.

34. Derynck, R., Feng, X. TGF-β receptor signaling. Biochem Biophys Acta; 1997: 1333:F105-F150.

35. Chen C, Knag Y, Massague J. Defective repression of c-myc in breast cancer cells: A loss at the core of the transforming growth factor β growth program. Proc Natl Acad Sci USA 2001;98:992-999.

36. Sun L, Chen C. Expression of transforming growth factor β type III receptor suppresses tumorigenicity of human breast cancer MDA-MB-231 cells. J Biol Chem 1997;272:25367-25372.

37. Chen C, Wang X, Sun L. Expression of transforming growth factor β (TGFβ) type III receptor restores autocrine TGFβ1 activity in human breast cancer MCF-7 cells. J Biol Chem 1997;272:12862-12867.

38. Prall OW, Rogan EM, Musgrove EA, Watts CK, Sutherland RL. c-Myc or cyclin D1 mimics estrogen effects of cyclinE-cdk2 activation and cell cycle reentry. Mol Cell Biol 1998;18:4499-4508.

39. Pietenpol J, Munger K, Howley P, Stein R, Moses HL. Factor-binding element in the human c-myc promoter involved in transcriptional regulation by transforming growth factor β1 and by the retinoblastoma gene product. Proc Natl Acad Sci USA 1991;88:10227-10231.

40. Sears RC, Nevins JR. Signaling networks that link cell proliferation and cell fate. J Biol Chem 2002;277:11617-20.

41. Trimarchi JM, Lees JA. Sibling rivalry in the E2F family. Nat Rev Mol Cell Biol 2002;3:11-20.

42. Majello B, De Luca P, Suske G, Lania L. Differential transcriptional regulation of c-myc promoter through the same DNA binding sites targeted by Sp1-like proteins. Oncogene1995;10:1841-8.

43. Oster SK, Ho CSW, Soucie EL, Penn LZ The *myc* oncogene: Marvelously Complex. Adv Cancer Res 2002; 84: 82-154.

44. Huang H-J, Yee J-K, Shew J-Y, Chen P-L, Bookstein R, Friedmann T. Suppression of the neoplastic phenotype by replacement of the RB gene in human cancer cells. Science 1988; 242: 1563-1566.

45. Liburdy RP, Callahan DE, Harland J, Dunham E, Sloma TR, Yaswen P. Experimental evidence for 60 Hz magnetic fields operating through the signal transduction cascade. Effects on calcium influx and c-MYC mRNA induction. FEBS Lett 1993;334: 301-308.

46. Wonderlin WF, Strobl JS. Potassium channels, proliferation and G1 progression. J Memb Biol 1996; 154: 91-107.

47. Mesra UK, Gawdi G, Pizzo SV. Chloroquine, quinine and quinidine inhibit calcium release from macrophage intracellular stores by blocking inositol 1,4,5-triphosphate binding to its receptor. J Cell Biochem 1997; 64:225-232.

48. Botos J, Smith R III, Kochevar DT. Retinoblastoma function is a better indicator of cellular phenotype in cultured breast adenocarcinoma cells than retinoblastoma expression. Exp Biol Med 2002; 227: 354-362.

Figure 1

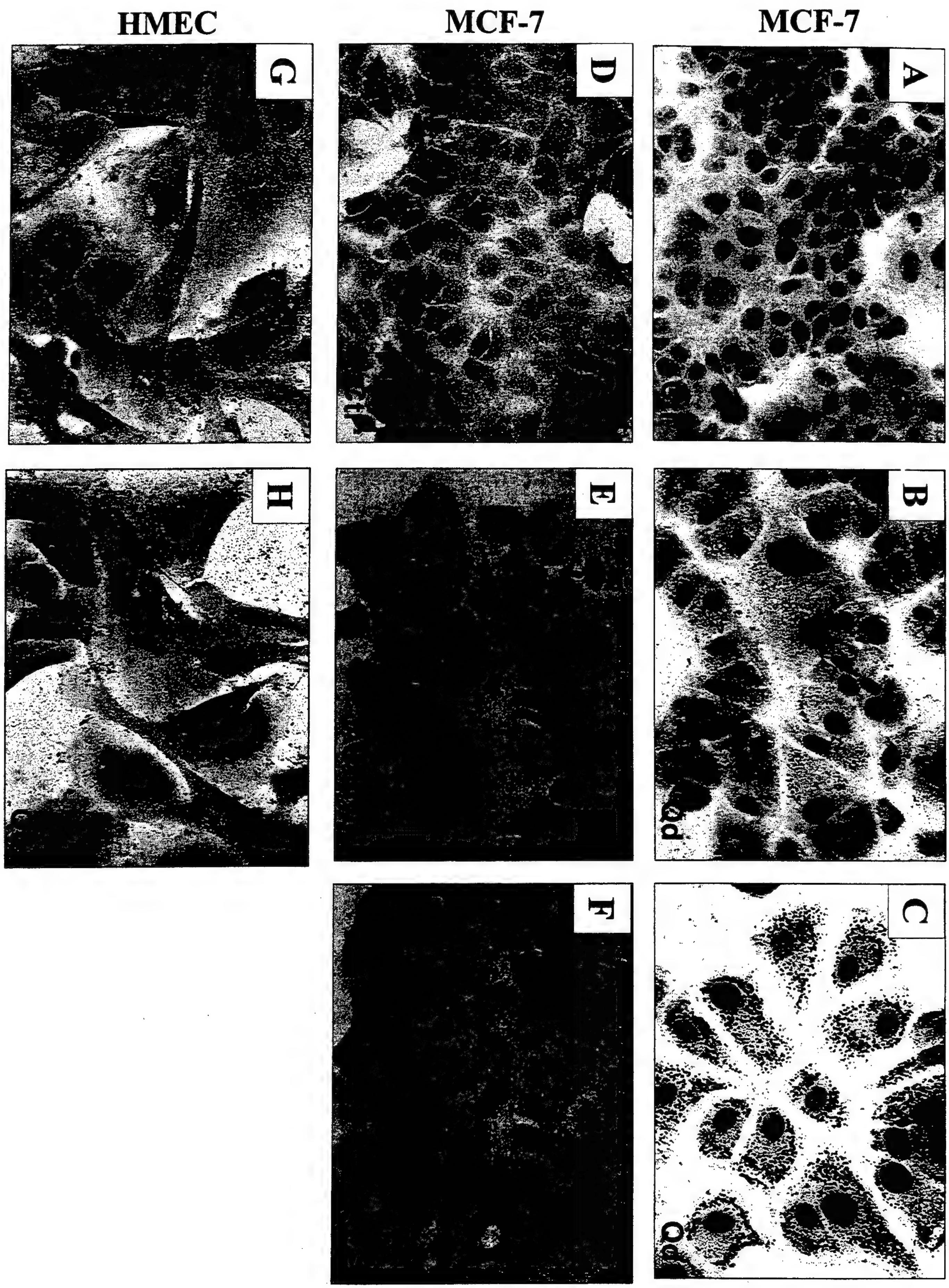

Figure 2

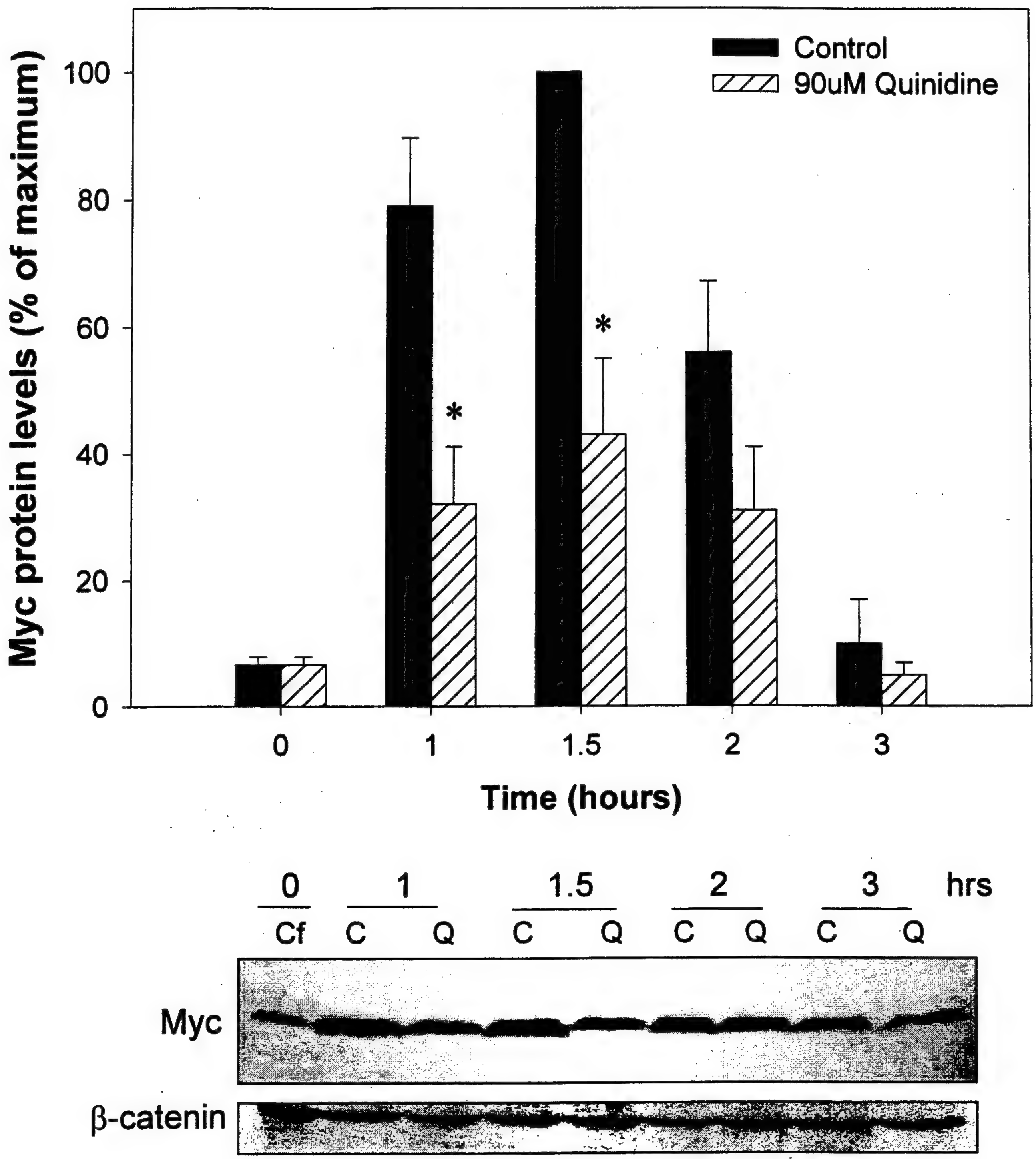
Control
90uM Quinidine
Myc protein levels (% of maximum)
100
80
60
40
20
0
*
*
0
1
1.5
2
3
Time (hours)
0
1
1.5
2
3
hrs
Cf
C
Q
C
Q
C
Q
C
Q
Myc
β-catenin

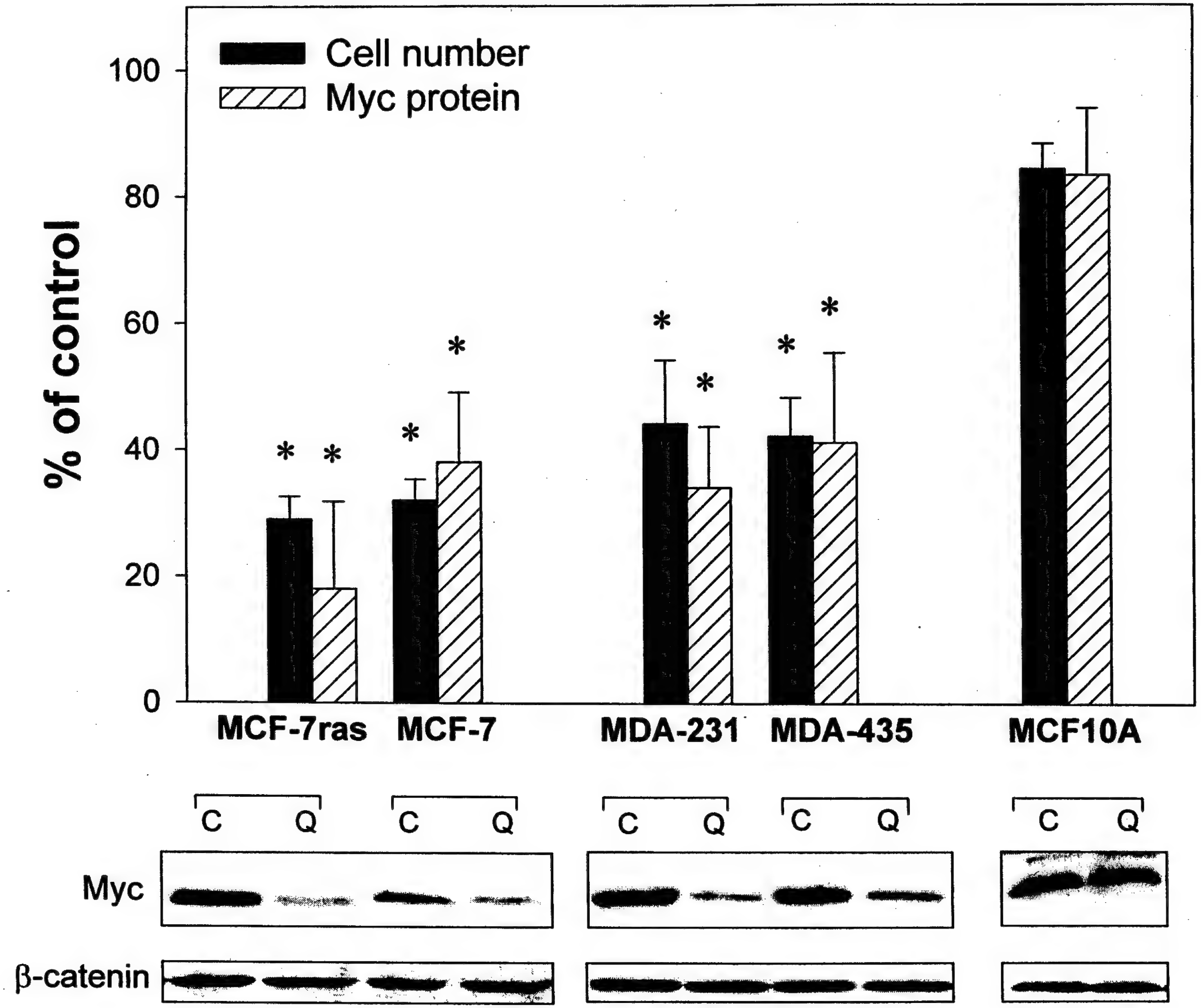
Cell number
Myc protein
% of control
100
80
60
40
20
0
MCF-7ras
MCF-7
MDA-231
MDA-435
MCF10A
C
Q
Myc
β-catenin

Figure 3

Figure 4

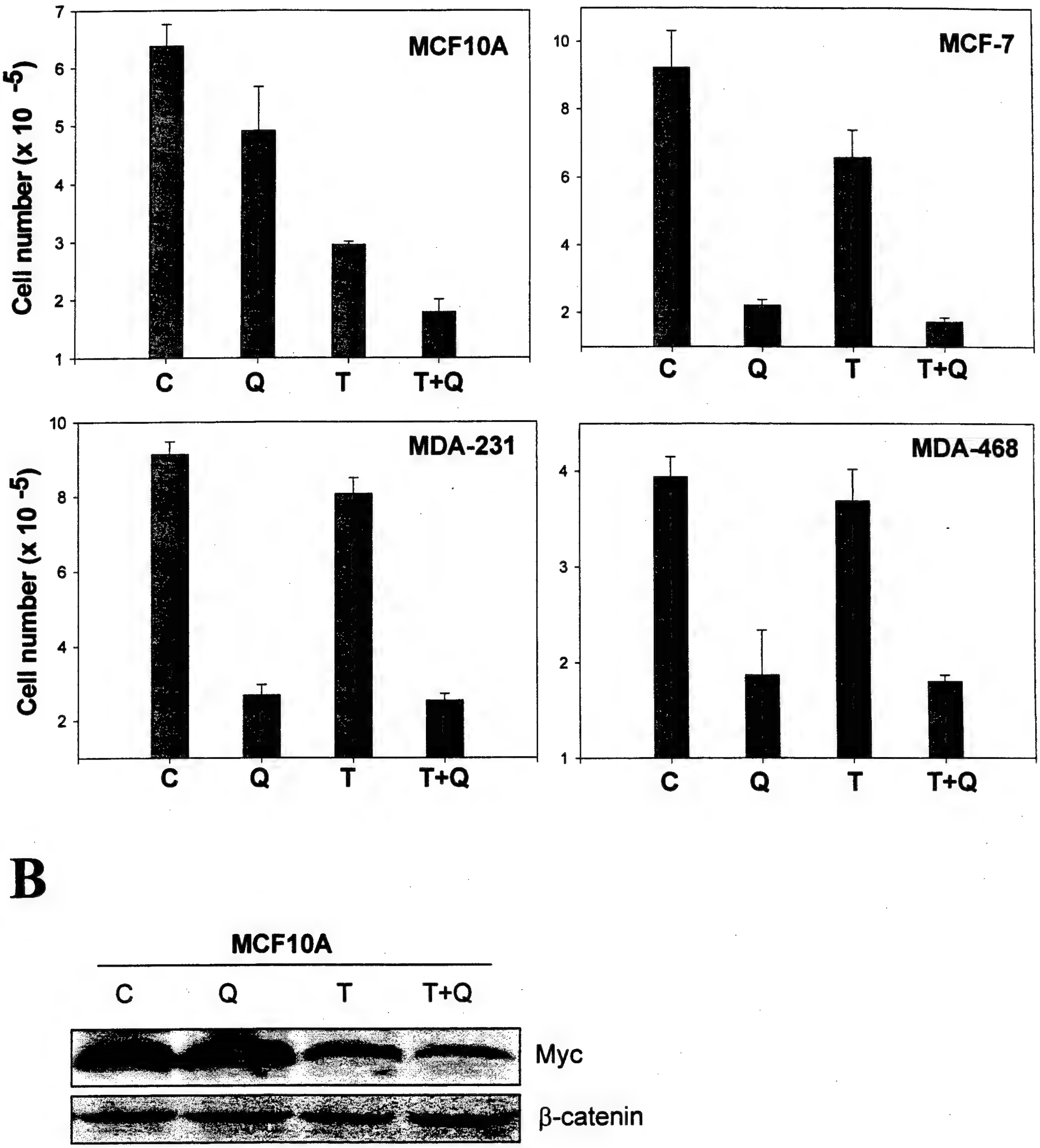

A
MCF10A
MCF-7
MDA-231
MDA-468
Cell number (x 10 -5)
Cell number (x 10 -5)
C
Q
T
T+Q
B
MCF10A
C
Q
T
T+Q
Myc
β-catenin

Figure 5

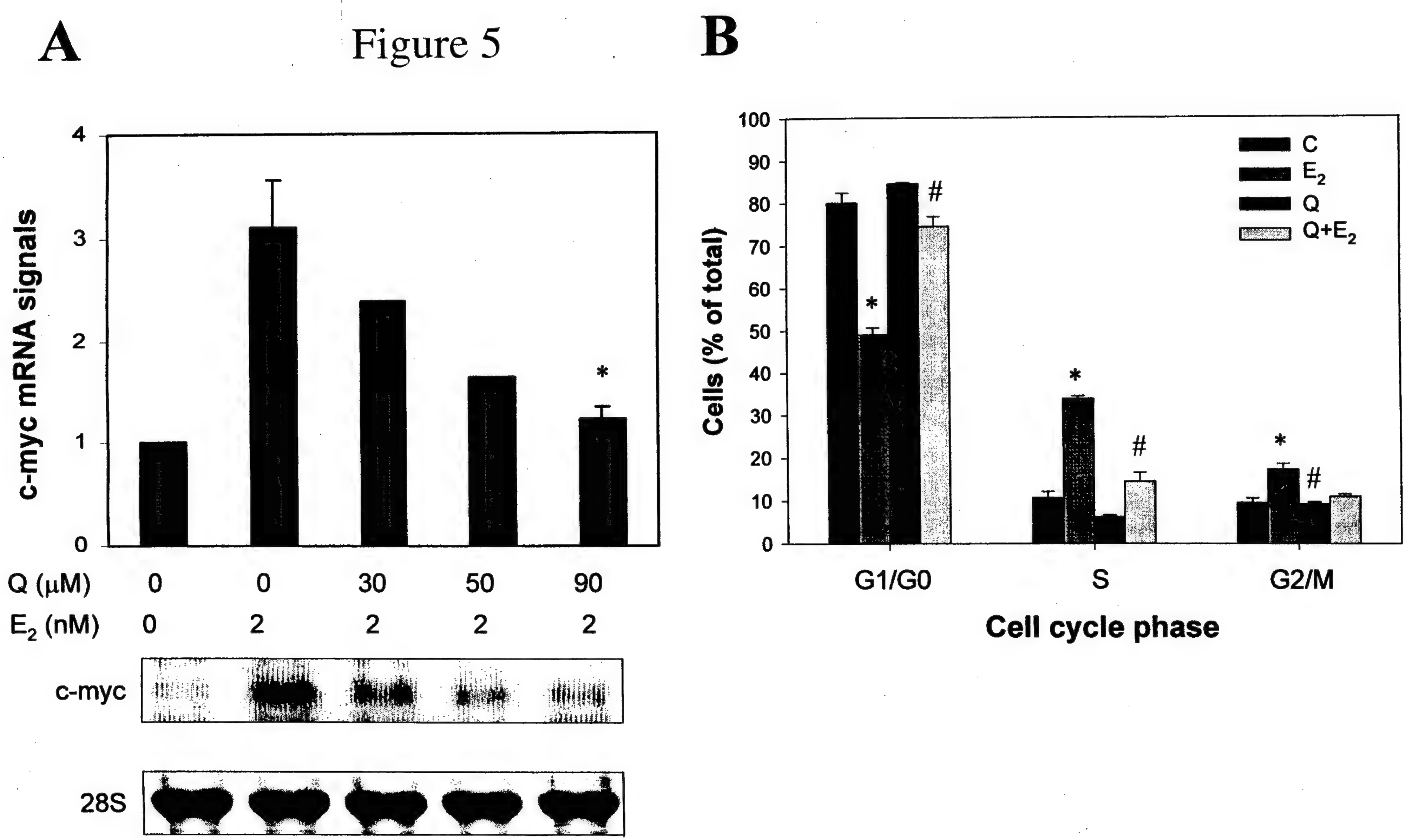
A
c-myc mRNA signals
0
1
2
3
4
Q (μM) 0 0 30 50 90
E2 (nM) 0 2 2 2 2
c-myc
28S
B
Cells (% of total)
0
10
20
30
40
50
60
70
80
90
100
C
E2
Q
Q+E2
G1/G0
S
G2/M
Cell cycle phase

Figure 6

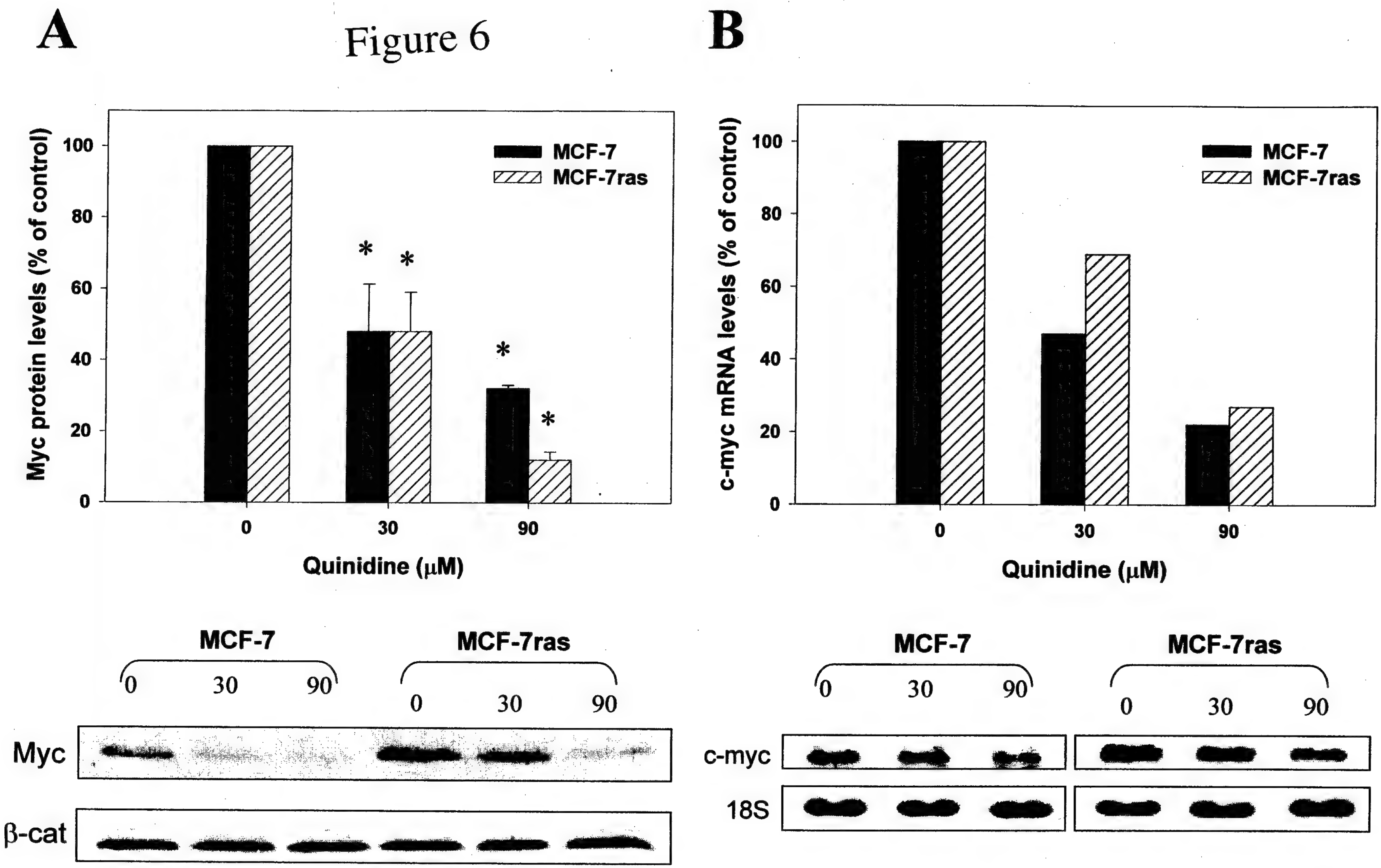
A
B
Myc protein levels (% of control)
100
80
60
40
20
0
MCF-7
MCF-7ras
*
0
30
90
Quinidine (μM)
c-myc mRNA levels (% of control)
MCF-7
MCF-7ras
0
30
90
0
30
90
Myc
β-cat
c-myc
18S

Figure 7

A

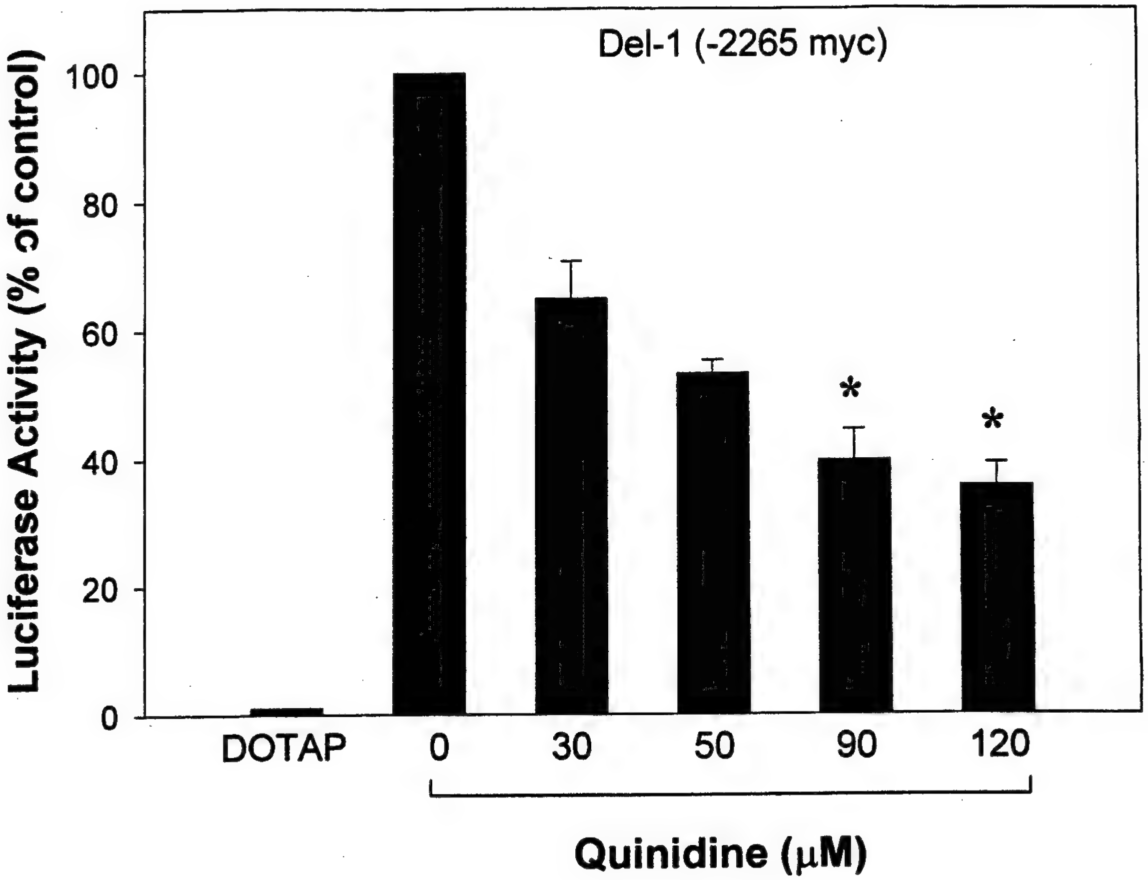

B

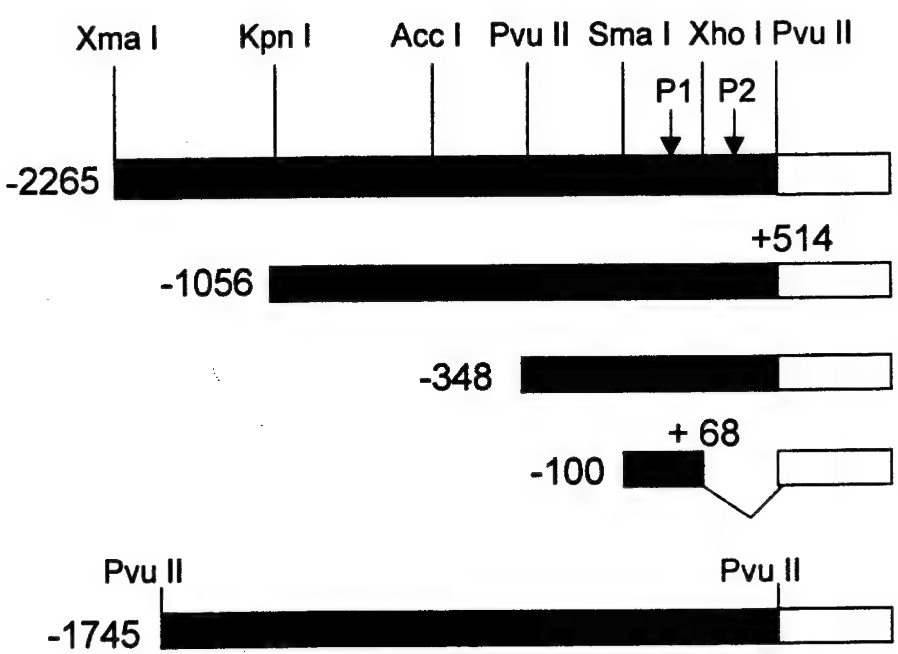

	C	Q	% Δ
Del-1	1	.33	67 ↓*
Del- 2	19	6.8	64 ↓*
Del- 4	27	8.7	68 ↓*
Frag-E	4.2	1.4	67 ↓*
CD1Luc	.93	1.1	20 ↑

Figure 8

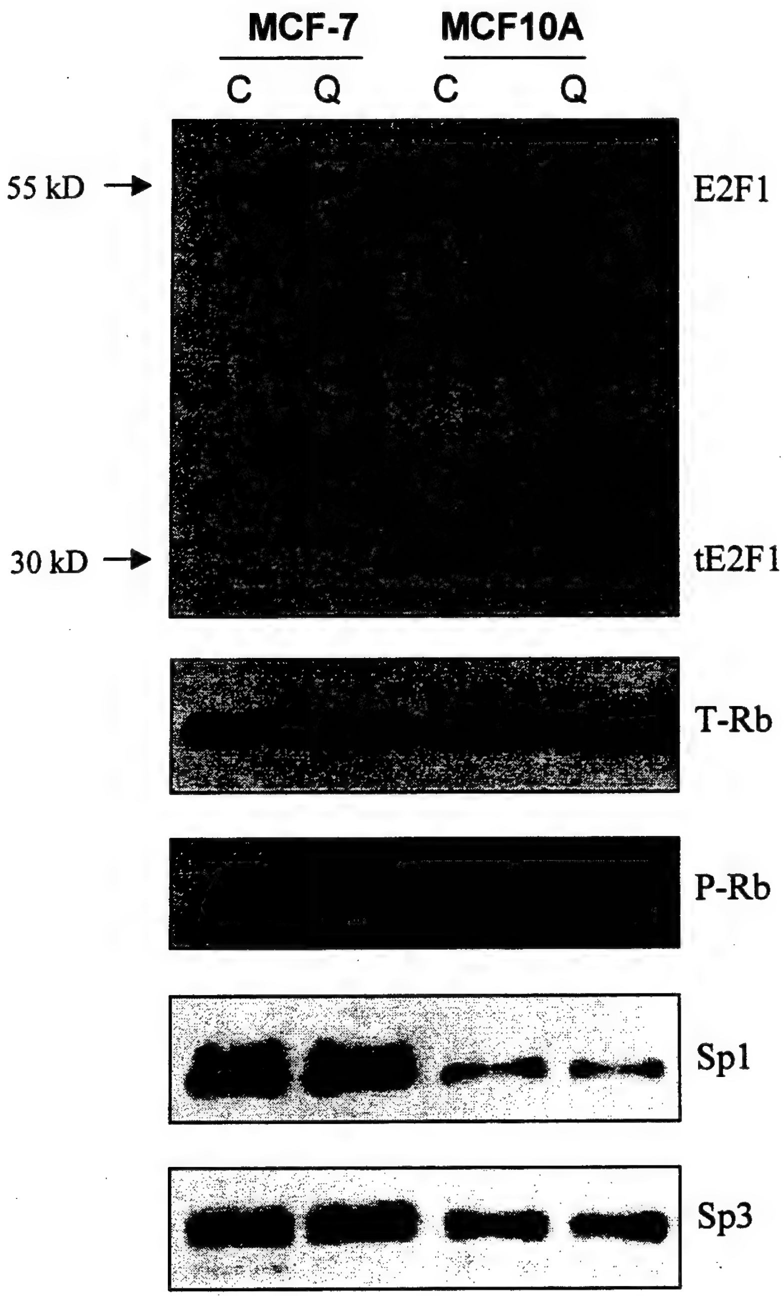

Figure 9

A

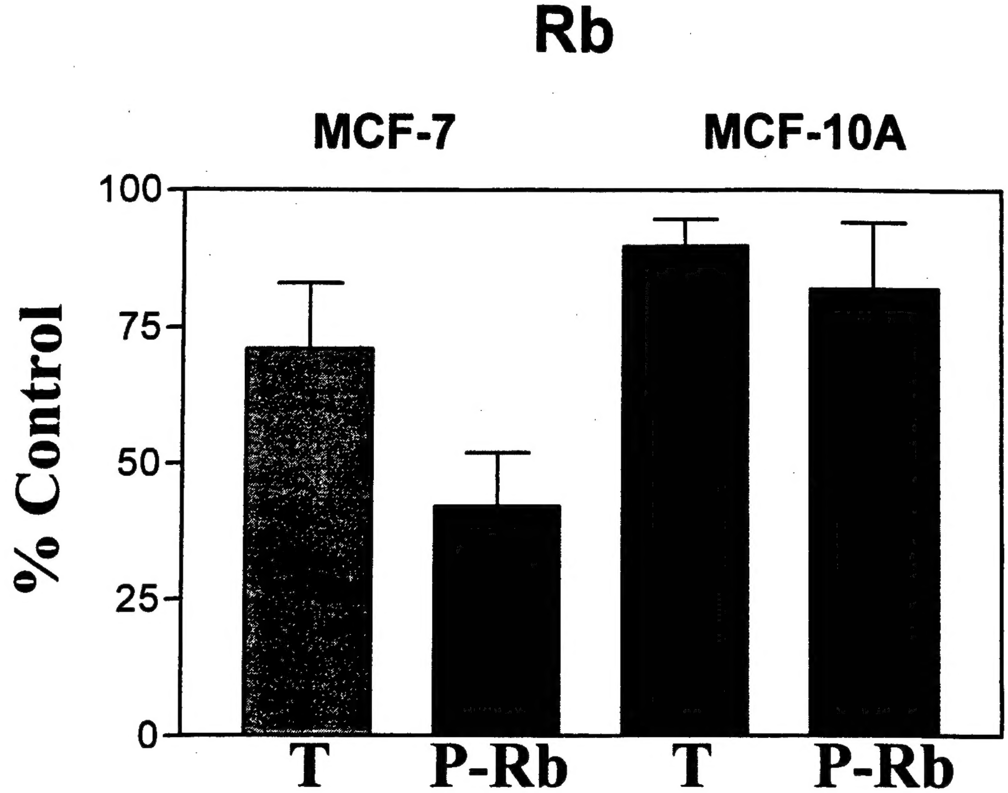
Rb
MCF-7
MCF-10A
100
75
50
25
0
% Control
T
P-Rb
T
P-Rb

B

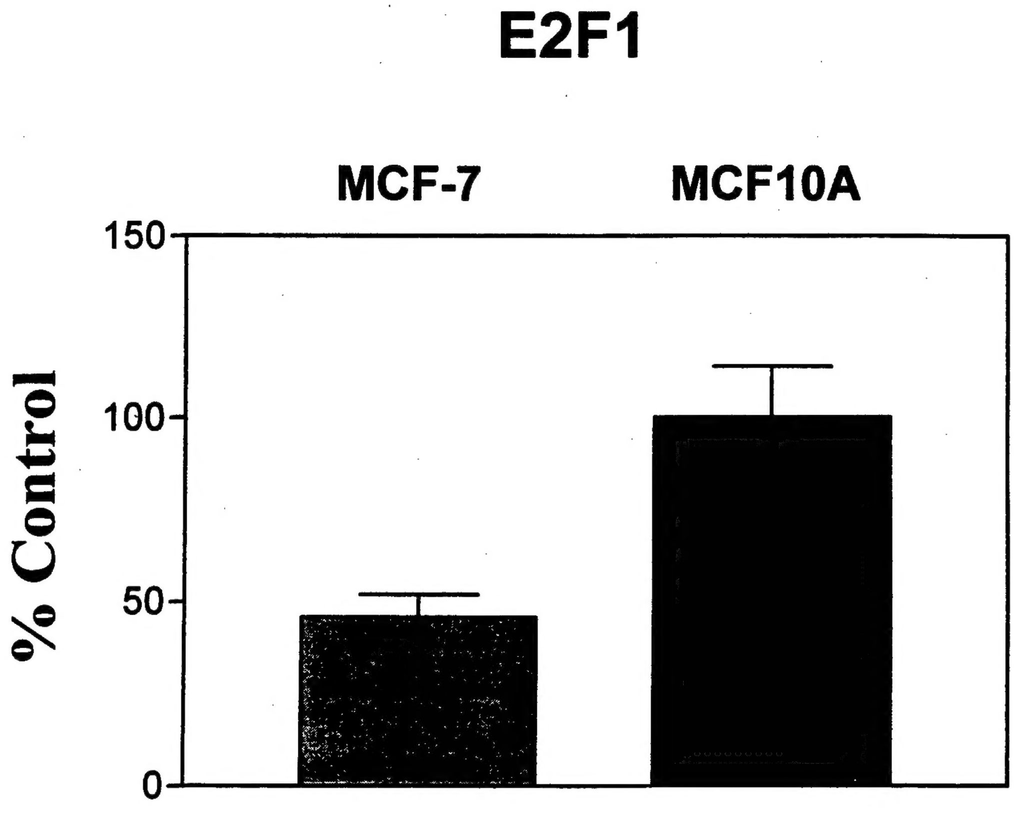
E2F1
MCF-7
MCF10A
150
100
50
0
% Control

New Pharmacologic Agents Promote Cell Differentiation in Human Breast Tumor Cells.

Anna Martirosyan, Qun Zhou, Rayhana R. Bata, Meredith A. McCracken[1], Andrew B. Freeman, Carla Morato-Lara, and Jeannine S. Strobl

Biochemistry & Molecular Pharmacology, Genetics & Developmental Biology Program[1], West Virginia University, Morgantown, WV 26506

Quinidine (QD) is a quinoline ring-containing drug which we showed previously to cause cell cycle arrest in G1, promote cell cycle exit as measured by loss of Ki67 antigen expression, and stimulate cellular differentiation in MCF-7 breast tumor cells. We hypothesized that the ability to arrest the cell cycle and induce cellular differentiation was shared by other pharmacologically active quinolines. Quinoline ring compounds (27) were obtained from NCI or Sigma. Effects on cell viability were screened using the tetrazolium dye metabolism (MTS) assay; we used the MTS IC50 value in subsequent assays. Lipid droplet accumulation was used to identify compounds with the potential to promote cellular differentiation. By these criteria, five NCI compounds were identified that stimulate differentiation of human breast cancer cell lines MCF-7 and MDA-MB-231: NSC4239 (0.7uM), NSC4238 (0.6uM), NSC10010 (3.6 uM), NSC86371 (5.5uM), and NSC2039 (10 uM). Certain quinoline antimalarials also stimulated MCF-7 cell differentiation: amodiaquin (7 uM), chloroquine (30 uM), quinine (40 uM), and hydroxychloroquine (57 uM). The ability of these compounds to promote exit from the cell cycle was monitored immunohistochemically by the loss of Ki67. Tumor cell differentiation agents can inhibit histone deacetylase (HDAC). Two of the new differentiating agents, NSC86371 and NSC~~2039~~ 3852 are novel direct HDAC1 inhibitors; the mechanism of action of the additional compounds is under investigation. We conclude that quinolines have interesting pharmacologic properties that promote breast tumor cell differentiation *in vitro*.

Supported by DAMD-17-00-1-0500, CAMC 8-2001, Mary Babb Randolph Cancer Center

transcription, and Myc is thought to regulate a specific subset of target genes that in turn regulates the biological activities of Myc. It is essential to identify the full complement of Myc regulated genes to truly understand the role of Myc within the cell. Despite extensive work in this area, relatively few bona fide target genes have been identified to date.

To this end, we have undertaken a microarray approach to identify Myc regulated genes. cDNA prepared from Myc-/- and Myc+/+ cells was hybridized in duplicate to a microarray which contained known cDNAs and unknown ESTs. Putative regulated genes were identified and subjected to additional rounds of screening to identify bona fide Myc regulated genes. The criteria used to assess true Myc regulated genes was extensive and accomplished using a repertoire of experimental tools. These included inducible Myc expression systems to chromatin immunoprecipitation experiments. Interestingly, by analyzing each putative regulated gene in these screens we were able to exclude many targets that were regulated as a consequence of cell cycle progression and not solely as a result of Myc expression. With these bona fide Myc target genes in hand we have the experimental tools necessary to assess both the mechanism of Myc regulation of gene transcription and the role these target genes hold in regulating the diverse biological activities downstream of Myc.

68

C-MYC Amplification is a Feature of *BRCA1*-associated Hereditary and *BRCA1*-methylated Sporadic Breast Cancers

Tatyana A. Grushko[1], Soma Das[2], Philip L. Schumm[3], April J. Adams[1], Lise Sveen[1], Kristin Anderson [1], Fitsum Hagos[1], Olufunmilayo I. Olopade[1], [1]Department Medicine, Section Hematology/Oncology, University of Chicago, 5841 S. Maryland Ave, Chicago, IL 60637, [2]Department of Human Genetics, University of Chicago, [3]Department of Health Studies, University of Chicago

Breast cancer is a heterogenous disease caused by the progressive accumulation of genetic changes in a growing number of oncogenes and tumor suppressor genes. Germ-line mutations in the *BRCA1* tumor suppressor gene result in breast cancers characterized by young age of onset, estrogen receptor negativity (ER-), and a distinctly high-grade tumor phenotype. Methylation of the *BRCA1* promoter occurs in 7-31% of breast tumors and may be an important mechanism for functionally inactivating *BRCA1* in sporadic breast cancers. Presumably *BRCA1*-methylated sporadic cancers display similar gene-expression profiles to *BRCA1*-associated hereditary breast cancers. C-MYC interacts with the BRCA1 protein, and the oncogene is amplified in 5-50% of breast cancers. To assess the contribution of *C-MYC* amplification to the aggressive biology of *BRCA1*-associated or *BRCA1*-methylated tumors, we performed FISH using *C-MYC* assay on formalin-fixed paraffin-embedded tumor tissues from women with known deleterious *BRCA1* mutations or hypermethylation of the *BRCA1* promoter. To date, we have observed a *C-MYC/CEP8* amplification ratio > 2 in 13/21 (62%) *BRCA1*-associated and in 4/8 (50%) *BRCA1*-methylated tumors, including 6 tumors with ratios > 4. Our data suggest that *C-MYC* amplification occurs in a significant proportion of tumors with *BRCA1* dysfunction. Thus, it is likely that *C-MYC* amplification contributes to the aggressive histological features observed in these tumors.

Supported by an Academic Award from the US Army Department of Defense grant DAMD17-99-1-9123 and by a grant from the Falk Medical Research Trust.

69

Reciprocal relationship between phosphorylation and O-GlcNAcylation at Thr58 on c-Myc

Kazuo Kamemura, Bradley K Hayes, Frank I Comer, Gerald W Hart, Department of Biological Chemistry, Johns Hopkins University School of Medicine, 403 Hunterian Bldg., 725 N. Wolfe Street, Baltimore, MD 21205-2185

O-linked N-acetylglucosamine (O-GlcNAc) is an abundant posttranslational modification of nuclear and cytoplasmic proteins in eukaryotes. Virtually all known O-GlcNAcylated proteins are also phosphoproteins that form reversible multimeric protein complexes, suggesting that O-GlcNAc may modulate protein phosphorylation, protein-protein interaction, or both. c-Myc is a helix-loop-helix leucine zipper protein that regulates gene transcription in cell proliferation and apoptosis. Thr58 within the N-terminal transactivation domain of c-Myc has been independently identified as both an O-GlcNAcylation and phosphorylation site. Thr58 is also a known mutational hot spot in lymphomas and this mutation is thought to be involved in tumor progression. This evidence lead us to the hypothesis that these two post-translational modifications of Thr58 regulate c-Myc's function differentially. Here we present evidence for a functional relationship between phosphorylation and O-GlcNAcylation at Thr58. First, we describe the production and characterization of two antibodies. One specifically reacts with the Thr58-O-GlcNAcylated form of c-Myc and the other reacts with unmodified Thr58 on c-Myc. Using these antibodies together with a commercial anti-phospho-Thr58 antibody, we detected simultaneously three forms of c-Myc (Thr58-unmodified, -phospho, and -glyco forms) in HL60 and HEK293 cells. A candidate for the kinase responsible for Thr58 phosphorylation is the glycogen synthase kinase (GSK3). By treatment of the cells with lithium, a competitive inhibitor of GSK3, we observed a decrease of the phospho form and an increase of both glyco and unmodified forms. This suggests that O-GlcNAcylation and phosphorylation at Thr58 occur reciprocally. Because phosphorylation at Thr58 is thought to be associated with a negative regulation of c-Myc, O-GlcNAcylation may play a positive role in the regulation of the functions of c-Myc.

70

Suppression of c-Myc Protein and Induction of Cellular Differentiation in Human Breast Cancer Cells but not in Normal Human Breast Epithelial Cells by Quinidine

Zara K Melkoumian[1], Meredith A McCracken[2], Jeannine S Strobl[1], [1]Biochemistry and Molecular Pharmacology, West Virginia University, R.C. Byrd HSC, Morgantown, WV 26506, [2]Genetics and Developmental Biology Program, West Virginia University

C-myc protooncogene plays an important role in cell cycle progression, cellular differentiation and apoptosis. Abnormal expression of the c-myc gene was reported in 32% of breast cancers, implying it is important in the genesis and/or progression of breast cancer. Suppression of c-myc by antisense oligonucleotides inhibits growth in MCF-7 and MDA-231 human breast cancer cell lines [Watson, P.H. et al, Cancer Res, 51:3996-4000, 1991]. In our previous studies we showed down-regulation of c-myc mRNA levels and promoter activity, G1/G0 arrest and inhibition of growth in MCF-7 cells in response to quinidine. Here we report rapid within 1 to 2 hours down-regulation of Myc protein in a panel of breast cancer cell lines (MCF-7, MCF-7ras, MDA-231, MDA-435) treated with quinidine. Myc suppression was sustained (at least 24 hrs) and was followed by inhibition of growth and induction of a more differentiated phenotype in the described cell lines. Interestingly, quinidine did not have any effects on Myc protein levels or proliferation in the MCF10A normal human mammary epithelial cell line. The effects of quinidine on Myc were not mediated through the TGFbeta1 pathway. Jointly, these results suggest that quinidine selectively suppresses Myc protein levels and induces differentiation in the breast cancer cells but not in the normal breast epithelial cells.

Supported by DAMD 17-99-1-9447, DAMD 17-99-1-9449, DAMD 17-00-1-0500.

71

N-Myc overexpression leads to decreased b1 integrin increased apoptosis in human neuroblastoma cells

Cynthia M van Golen[1], Daniel Noujaim[1], Valerie P Castle[2], [1]Neurology, University of Michigan, 200 Zina Pitcher Pl., 4414 Ann Arbor, MI 48109-0588, [2]Pediatrics and Communicable Dis of Michigan

Neuroblastoma is a childhood tumor of the peripheral nervous s arise through improper differentiation of neural crest cells. MYCN, leading to increased expression of the gene product l poor patient prognosis, although the mechanism of action of largely unknown. N-myc has been shown to increase cell growth like growth factor type I receptor (IGF-IR), and increase combination with Bcl-2. The current study investigates the affi apoptosis, cell signaling, and adhesion protein expression. Despit Myc on cell growth, N-Myc overexpression in SHEP neu (SHEP/N-Myc cells) also increases serum-withdrawal induced apoptosis. We have previously shown a protective effect of IGF-I in SHEP cells undergoing either serum-withdrawal-induced or mannitol-induced apoptosis. However, although SHEP/N-Myc cells have increased IGF-IR expression, IGF-I rescue from these apoptotic stimuli is prevented. The two predominant signaling pathways downstream from the IGF-IR result in Akt or ERK1/2 phosphorylation. Neither of these pathways is affected by N-Myc overexpression in SHEP cells. Observations of N-Myc overexpression SHEP cells (SHEP/N-Myc cells) revealed that these cells became less adherent in culture. SHEP/N-Myc cells have dramatically less b1 integrin expression than control cells, consistent with previous reports in the literature. b1 integrin expression is decreased in more tumorigenic neuroblastoma cells lines, including IMR32 and SH-SY5Y cells. N-Myc promotes growth on a fibronectin substrate, but leads to decreased growth on plastic. Finally, N-Myc increases the number of cells in S phase, which is prevented by ERK1/2 inhibition. . We speculate that the decrease in b1 integrin expression leads to a less differentiated phenotype, resulting in increased growth and tumorigenesis proper conditions, or leading to apoptosis if deprived of growth sustaining molecules.

72

Smad3 Recruits the Anaphase Promoting Complex for Ubiquitination and Degradation of SnoN

Shannon L Stroschein[1], Shirin Bonni[2], Jeffrey L Wrana[2], Kunxin Luo[1], [1]Molecular and Cell Biology, Univ. of California-Berkeley, 229 Stanley Hall #3206, Berkeley, CA 94618, [2]Molecular Biology and Cancer, Mount Sinai Hospital, Canada

Smad proteins mediate transforming growth factor-ß (TGFß) signaling to regulate cell growth and differentiation. SnoN is an important negative regulator of TGFß signaling that functions to maintain the repressed state of TGFß target genes in the absence of ligand. Upon TGFß stimulation, Smad3 and Smad2 translocate into the nucleus and induce a rapid degradation of SnoN, allowing activation of TGFß target genes. Here we show that Smad2- or Smad3-induced degradation of SnoN requires the ubiquitin-dependent proteasome and can be mediated by the anaphase promoting complex (APC) and the UbcH5 family of ubiquitin conjugating

NOVEL BREAST TUMOR DIFFERENTIATION AGENTS

Strobl, J.S., Zhou, Q.,and Martirosyan, A.

West Virginia University

jstrobl@hsc.wvu.edu

The use of breast tumor differentiating agents to complement existing therapies has the potential to improve breast cancer treatment. We are investigating the use of antimalarials as breast tumor differentiation agents on the basis of previous work showing that quinidine induces differentiation and apoptosis in human breast tumor cells in vitro. To test whether antitumor activity was a general property of antimalarial agents, we screened a panel of quinidine analogs. We found that MCF-7 cell exit from the cell cycle into G0, marked by a loss of Ki67 antigen expression, was a typical response to antimalarial drugs. The rank order of potency for MCF-7 cell growth inhibition (MTS. IC50) in a series of antimalarials showed quinidine was the least potent among common antimalarial agents: primaquine (3 uM)<amodiaquin (7 uM)< halofantrine (10 uM)< chloroquine (35 uM)< quinine (40 uM) < quinidine (110 uM). These antimalarial agents also increased acetylated histone H4 levels in MCF-7 cells a response that is associated with differentiation in human breast tumor cells. We suggest that antimalarials raise histone H4 acetylation levels by a novel mechanism, because none of the antimalarials were direct inhibitors of HDAC 1/ 2 activity. Although all the antimalarials tested elicited two novel and significant antitumor responses in MCF-7 human breast tumor cells, histone H4 hyperacetylation and cell cycle exit into a non-proliferative (G0) state, only quinidine and chloroquine stimulated apoptosis in MCF-7 cells. To search for more potent structural analogs of chloroquine with similar antitumor responses in MCF-7 cells, approximately twenty amino alkyl substituted quinoline ring compounds from the NCI Compound Library were screened for growth inhibition (MTS IC50) and cell cycle exit (Ki67 index). NCI 4238 and NCI 10010 inhibited cell survival at sub-micromolar concentrations. stimulated exit from the cell cycle (Ki67 index), and promoted morphological changes typical of differentiating breast tumor cells. In summary, antimalarial agents and structural analogs exhibit antitumor properties in human breast cancer cells in vitro that are consistent with a novel mechanism of action as breast tumor cell differentiating agents.

The U.S. Army Medical Research Materiel Command under DAMD17-00-1-0500